massachusetts institute of technology — artificial intelligence laboratory

Design and Control of an Anthropomorphic Robotic Finger with Multi-point Tactile Sensation

Jessica Lauren Banks

AI Technical Report 2001-005 May 2001

Design and Control of an Anthropomorphic Robotic Finger with Multi-point Tactile Sensation

by

Jessica Lauren Banks

B.S., University of Michigan (1994)

Submitted to the Department of Electrical Engineering and Computer Science in partial fulfillment of the requirements for the degree of

Master of Science

at the

MASSACHUSETTS INSTITUTE OF TECHNOLOGY

May 2001

Certified by: Rodney A. Brooks
Professor, Department of Electrical Engineering and Computer Science
Thesis Supervisor

Accepted by: Arthur C. Smith
Chairman, Department Committee on Graduate Students

Design and Control of an Anthropomorphic Robotic Finger with Multi-point Tactile Sensation

by

Jessica Lauren Banks

Submitted to the Department of Electrical Engineering and Computer Science on May 11, 2000, in partial fulfillment of the requirements for the degree of Master of Science

Abstract

The goal of this research is to develop the prototype of a tactile sensing platform for anthropomorphic manipulation research. We investigate this problem through the fabrication and simple control of a planar 2-DOF robotic finger inspired by anatomic consistency, self-containment, and adaptability. The robot is equipped with a tactile sensor array based on optical transducer technology whereby localized changes in light intensity within an illuminated foam substrate correspond to the distribution and magnitude of forces applied to the sensor surface plane [58].

The integration of tactile perception is a key component in realizing robotic systems which organically interact with the world. Such natural behavior is characterized by compliant performance that can initiate internal, and respond to external, force application in a dynamic environment. However, most of the current manipulators that support some form of haptic feedback either solely derive proprioceptive sensation or only limit tactile sensors to the mechanical fingertips. These constraints are due to the technological challenges involved in high resolution, multi-point tactile perception.

In this work, however, we take the opposite approach, emphasizing the role of full-finger tactile feedback in the refinement of manual capabilities. To this end, we propose and implement a control framework for sensorimotor coordination analogous to infant-level grasping and fixturing reflexes. This thesis details the mechanisms used to achieve these sensory, actuation, and control objectives, along with the design philosophies and biological influences behind them. The results of behavioral experiments with a simple tactilely-modulated control scheme are also described.

Thesis Supervisor: Rodney A. Brooks
Title: Professor, Department of Electrical Engineering and Computer Science

Acknowledgments

A wise advisor once told me that I "write like a German philosopher." Hopefully, I will be better at articulating my thanks to all those people who coached me on the finer technical and mental points that led to this thesis.

I am eternally grateful to Rod Brooks for letting me work under the auspices of his notoriety, I mean, prestige. He has created a research environment free of boundaries and never ceases to straighten the Wondrous Big Picture for me when it gets knocked askew (or tilt it when it gets too straight).

Thank you to Rob Inkster, David Lockhorst, and the rest of the gang at Tactex as well as Ernie Riemer at Canpolar, without whose generous help, interest, and resources, I could have never done this research.

I am indebted to Aaron Edsinger who has been a surrogate supervisor to me (in exchange for scavenged treasures). He is my real life robotboy and always amazes me with his generosity and genius.

A big old thanks to Beep (Bryan Adams) who generally went above and beyond the call of T.A. duty to relieve some of my stress—and be so lovingly the brother I never wanted. You have definitely earned your 90-minute wings.

Thank you to my officemates, Paulina Varchavskaia and Eduardo Torres-Jara, who have put up with my whining and always watched over me while I napped on the futon. ThanX to the stylings of maX, who kept me company (and kept me sane) during long nights at the lab. A big hug goes out to the other AI "support" staff who make the lab a home away from home (minus the showers and plus the candy machines): Una-May O'Reilly, Cynthia Breazeal, Charlie Kemp, Lijin Aryananda, Brian Scassellati, Matt Marjanovic, Juan Velasquez, Paul Fitzpatrick, Artur Arsenio, Sally Persing, Annika Pfluger, and Ron Wiken. (Oh, and thanks to those candy machines.)

I really cannot imagine making it through this time (or any particular day, to say the least) without the constant patience, care, and help of Dan Paluska. I love you. And now it's in print.

And finally, thank you to my parents, Seth and Jeri Banks, and my sister, Becca, whose confidence in me never wavered. I simply could not have done this work, let alone be the person capable of doing it, had they not been so supportive. I love you.

Contents

List of Figures

List of Tables

Chapter 1

Introduction

1.1 Problem Overview

The human hand can serve as a model for a robotic interface with the environment. With over twenty-five degrees of freedom (DOF), its versatility provides motivation for artificial manipulation research.

While the prehension and restraint capabilities of the human hand are objectives for industrial end-effectors, its manipulative and perceptive abilities prescribe basic determinants for medical, entertainment, and service systems. These applications require robots to perform anything from everyday activities to hazardous manual tasks. Prosthetic and tele-operated manipulators must possess many of these manual faculties because their control greatly relies on the mapping of a human user's natural conduct. Hands for humanoid robots must also express such compatibility if they are to promote intuitive human interaction and if developers are to converge on reliable research platforms.

Articulated hand functionality still remains a remote benchmark for engineering sophistication. Human hand strength and dexterity involve a complex geometry of cantilevered joints, ligaments, and musculotendinous units that must be analyzed as a coordinated entity. This evaluation is complicated by the lagging development of in vivo muscle force assessment techniques. Furthermore, the indeterminate problem posed by the redundancy of the muscles which generate forces across joints and tissues means that many quantitative solutions to hand dynamics are still pending [6].

The intricate mechanics of the hand is not the only factor behind its functional uniqueness. Our repertoire of movements is guided by cognitive representations of external stimuli provided to the brain by

our somatic sensory system. Cutaneous and kinesthetic neural afferent relays provide us with information about physical parameters of the world and the state of our bodily interactions within them. We can, for example, acquire data about the dimensionality, weight, position, composition, shape, and thermal conductivity of objects we touch. When exploited as feedback by our sensorimotor system, this tactilokinaesthetic, or *haptic*, perception leads to the manual dexterity which appears to have been intrinsically related to hominid evolution [12, 6].

Judging from these characteristics, it is no surprise that many initial forecasts about the rapid conception of highly adaptable, sensor-based robot hands have proven overly optimistic. For the most part, examples of such devices are still confined to the research laboratory. It is clear that a composite analysis of hand function can only be achieved through the collaborative efforts of many disciplines—implying in turn, that realization of a robotic analog requires the interaction of mechanisms for perception, sensorimotor coordination, and motor control. From an engineering standpoint, such system-wide interdependence poses a daunting challenge, not to mention the difficulties posed by each individual subsystem. Thus, many attempts to derive agile artificial hands have been application driven, concentrating on only isolated, practical features (see Section 1.2). Trade-offs for lower system complexity come at the expense of manipulator dexterity. Moreover, the lack of adequate *tactile* sensing seems to be a major shortcoming for robust manipulation control.

On a broad level, interest in active tactile force detection (half of the haptic sensing suite) has been slow-growing since its early infancy in the late 70's [52]. For one, this is because it was not originally perceived as critical to early generations of industrial *machines*. (Even our neighboring Draper Laboratory strongly contested the development of actively sensing robots [53]!) Such deterred economic justification relegated tactile applications to the advanced *robots* of AI intended for operation in unstructured environments and for sharing space with or substituting for people. Tactile devices must often make direct contact with sharp, hot, unstable environments. The search for sensitive materials that could also endure such menaces has also slowed the progress of artificial taction. Plus, the fragmentary understanding of human tactile perception has been a problematic metric for emulation.

At the research level, most groundwork on the subject dealt with processing static tactile images, following in the footsteps of early machine vision work. But much of our aptitude for manual exploration, recognition, and retention relies on active tactile sensing, especially in situations where visual input is restricted. Furthermore, if a current

hand platform *does* support such active sensing, it is usually limited to the fingertips [15, 69, 5, 82, 101, 100]. This runs counter to the distributed nature of our tactile apparatus; and only a class of human grasp configurations involves just the fingertips (see Figure 3.2). Thus, even from developments in active sensing, a definitive technique for multi-point superficial force detection has yet to emerge (see *Chapter 4*). Even though system performance specifications [53] have been delineated and many materials, devices, and data analysis methodologies have been surveyed [93, 49, 81], the present market for robot tactile sensing devices remains marginal and expensive.

The primary aim of this work is to develop basic hardware and software instruments that could lead to a tactually sensate platform for dextrous manipulation. The final result is intended to be applied to the humanoid robot, Cog, of the MIT Artificial Intelligence (AI) Lab (Figure 1.1). In conjunction with the physical system, this text endeavors to frame some of the redundancy, complexity, and distributed control challenges involved in the artificial emulation of human hand function and perception. With each finger as complex as many robot arms, the hand multiplies design and control issues. This work attempts to sidestep some of these obstacles by focusing on the construction of a planar robotic finger equipped with active multi-point taction based on Kinotex™ technology [58] (see *Chapter 4*). We take on the overall sensorimotor integration problem by implementing a building block for a manipulator that demonstrates some of the initial functionality of a human baby's hand. Besides performing a variety of grasps itself, the robot serves as a stepping stone for implementation of other, more complex actions that involve sensing and actuation of multiple fingers. In order to ensure that our robot finger could be replicated, modified, and incorporated into a multi-digit hand applicable to a humanoid, its architecture was influenced by self-containment, adaptability, and anthropomorphism.

1.1.1 Self-containment

One of the biggest obstacles confronted by designers working with inorganic materials to achieve the functionality of a human hand is that of consolidating actuators, drive systems, power sources, joints, and sensors into a maintainable, compact design. For prostheses and humanoid robots in particular, the housing must correlate with the shape and size of a real hand. An end-effector that is too heavy or cumbersome will not fare well when mounted on the end of a further articulated robot arm or in limited access spaces. Furthermore, if the manipulator is

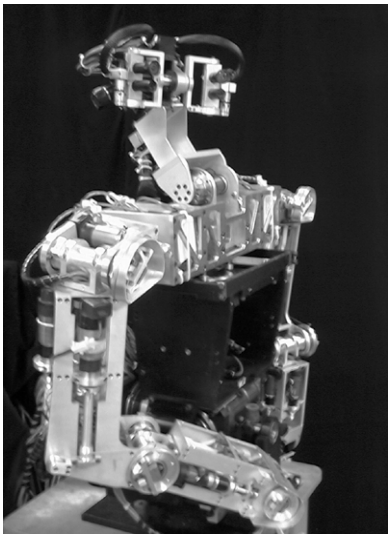

Figure 1.1: The humanoid robot, Cog, at the MIT AI Lab.

meant for a humanoid robot, the hand must be in proportion with, and any of its external drive components must be assimilated into, the rest of the body.

Traditional actuator technologies have a hard time rivaling the lightweight, compact form factor of organic muscle [83, 74, 25, 56, 90]. The high power-to-mass ratio that typifies muscle is a vital requirement for the mechanical actuation systems of autonomous and highly articulated robots. Moreover, that this ratio should include the mass of the energy source, makes muscle, with its efficient corporeal power supply, a model for comparison. These factors determine the speed and force generated through the transmission system of a given design.

If nature's experience sets the precedent, then actuators that can be scaled by parallel configurations of smaller units and located remotely from joint axes are appropriate. The finger described in this thesis approximates this through the use of miniature motors which drive the joints via bidirectional cable transmissions. The cables are routed through the hollows of the finger links and multiple motors can be contained within the profile of a hand. This is in contrast to having the actuators even further from the fingers (like the finger extensors and flexors originating in the human forearm) which would require routing the cables through the wrist, sacrificing power transmission and increasing the potential for cable wear. Also, by coupling the

distal and middle phalanxes, the design exploits the mobility of three linkages with only two motors. The control boards for the motors are modular as well and can be daisy-chained together (see *Chapter 3*). Because these boards are connected to the motors via ribbon cables, they can be positioned outside of the hand for further size and weight reduction.

Sensor integration experiences also reveal challenges associated with achieving the required capabilities within the desired size. The controller boards for our tactile sensors can be located remotely from the hand structure. This is due to the fact that their connections, which are the conduits for the tactile signals themselves, are flexible fiber-optic cables (see *Chapter 4*). As long as the angle of deflection is above a certain percentage of the fiber diameter, the signals will suffer no loss of integrity from being routed over long distances or through complex paths.

Special care was taken to choose materials and designs that would facilitate self-containment and modularity. These techniques should allow for different manipulators to be constructed with varying configurations and numbers of fingers as well as an engineered analog of a whole human hand. There was further incentive to investigate low-cost processes that would expedite mass production (at least relative to other robot fingers) and increase the opportunity for experimentation with different sensor arrangements.

1.1.2 Adaptability

For every dedicated task in which conventional end-effectors outperform a human hand, there are many more that they cannot even approximate. When the problem domain for a system extends over a broad spectrum of interactions—from handling massive objects to delicate, precise workmanship—the device is referred to as a "general-purpose manipulator" [49]. These manipulators support multi-modal sensory-actuation integration to react to task and object features by generating appropriate forces, configurations, and velocities. The ramifications of the dearth of such adaptable systems are becoming more pronounced in industry as well as in the AI community. Industrial arm-manipulator assemblies often necessitate the development of task-specific accessories to broaden their capabilities. Many times this requires process shutdown and operator intervention in order to change parts for the next step. Even worse, multiple equal, yet slightly modified, systems may have to run in series to do a job that a single general-purpose manipulator could manage. We believe it is possible and potentially very

profitable for robot hands to be able to wield tools designed for human use.

From the perspective of advanced engineering and artificial intelligence, the flexibility and compliance of the human hand is essential for developing service and personal robots which must perform in the dynamic environments of our homes and businesses. But task execution is not the only role human hands play in our relationship with the environment. They are modes of expression, protective barriers, and developmental accessories to the acquisition of body coordination and perceptual knowledge. Thus, an increasing demand for human-like manipulators arises from the field of AI, in which theories about or own cognitive development are being newly forged from and applied to the silicon and steel of humanoid entities.

The work of this thesis is greatly motivated by the need for system adaptability. We recognize that an anthropomorphic frameword is an unparalleled model of versatility, especially within the realm of a very human-moderated world. A robot must have a reliable means of obtaining feedback about the content of its surroundings in order to exhibit flexibility. We attempt to impart to the robot some of the qualities of human taction which enable our own adaptability. The incorporation of active, multi-point sensation is again of major import in this context, as it relays a comprehensive and dynamic representation of internally generated as well as externally imposed contact forces to the system. The general-purpose competence that this feedback bestows has led to our command over the local environment and our global assimilation to its changes.

1.1.3 Anthropomorphism

From the above descriptions, it is clear that biological consideration can be a valuable complement to the more technical strategies warranted by the design of artificially intelligent systems. Also referred to as a 'biomechanical', 'biomimetic', 'biomechatronic', or 'bionic' approach, the essential goal is to mechanically represent the function of living systems, either partially or totally.

In regard to this work on a component of a dextrous manipulator, some biological, specifically *anthropomorphic*, accommodation was almost compulsory, for we ultimately strive to achieve the abilities of the human hand. Reflection of human hand structure was also a priority because the final construction is intended for a humanoid robot. In the robotics community, however, the issue of whether such an end-effector needs to *look* human is unresolved. Yet, the form of the human hand is

an existence proof of a successful general-purpose manipulator design.

The physical structure of a humanoid component is not merely of practical consequence. The form of our bodies is considered by some to be inexorably linked to our mental interpretations of the world which shape our thoughts and even our language [66, 61]. A take on this concept is being studied at the MIT AI Lab, where research is infused with the premise that humanoid intelligence requires "a human like body in order to be able to develop similar sorts of representations" [17]. Thus, the work in this thesis stems from the belief that the development of cognitive processes is couched in the relationships between our perceptions, form, and function in the world.

Brooks has coined a concept that reflects this notion: *embodiment*. The embodiment of a creature defines its actions as "part of a dynamic with the world, having immediate feedback on the creature's own sensations through direct physical coupling and its consequences" [18]. As embodied beings, our morphology, sensorimotor system, and neurological apparatus, integrate empirical information that shapes our behavior—behavior which then in turn, over time, refines our initial brain and body structures. This happens on both an evolutionary scale and during an individual life span. So in building a robot that is to adhere, both physically and cognitively, to human-like performance, researchers must furnish it with some artificial perceptive faculties reminiscent of our own.

There are also other consequences of our embodiment. Much of our definitive humanness is the result of and dependent upon our interactions with other human beings. Therefore, an embodied humanoid should engage in, learn from, and rely on similar experiences. Seeking these relationships, however, is not necessarily an active responsibility of the artificial system. If such a system maintains an anthropomorphic identity then humans will be more inclined to relate naturally to it. In order for people to accept and integrate a robot into their lives, it should exhibit behavior (already said to rely heavily on form) that is intuitive and markedly congruent to our own. A disembodied creature does not inspire the spectrum of human interactions which are imperative for learning and development.

On an engineering level, the impact of embodiment becomes profound when working computer simulations (that are believed by many to be adequate evidence of a system's potential success) are translated into physical hardware. Depending on the complexity and intended autonomy of the system, this transition can be altogether futile. Accurately modelled kinematic creatures which work within idealized software environments are often undermined when physically introduced

into the cacophony of the world. This is due to inherent system noise and complicated external dynamics that cannot be generalized for every situation that the robot might encounter (e.g., variable friction, air resistance, magnetic fields, etc.) Lastly, in order to design systems that act like us, scientists must confront the philosophical, cognitive, sociological, etc. aspects that define "us." We feel the intellectual sharing among AI and other disciplines is further impetus to exercise the anthropomorphic approach.

Of course there are those who reject such methods, claiming that the basic aim of engineering is to solve mechanical problems, not to simulate people. And clearly, not all machine applications need comply with anthropomorphic consistency, especially because it basically defies the engineering maxims of simplicity and minimalism. On the other hand, as the economy, competition, and life-cycles of assembly line products change, an increasing need for robot flexibility arises even in venues where it was initially compromised. In both academia and industry, the potential of the approach is evidenced by the greater number of researchers that have imputed biological attributes to both hardware and software [70, 49, 71, 18, 100]. In terms of hardware, anthropomorphism can be expressed through physical geometry, actuation, and sensing. Marcinčin et al. [74] has referred to these instruments as "biomechanisms" and "biosensors." The former comprises ways to derive form from living constructs and to mechanically transduce energy into biologically based motion; the latter includes devices for actively obtaining empirical information about the surroundings in real-time.

From a software standpoint, biological resemblance can be used to implement modules for control, sensor integration, reasoning, learning, etc. Many different methods for carrying out these functions are present in the literature, for even at very primitive levels, the natural systems behind them are not fully comprehended. The fast, parallel integration and elaboration of sensory information inherent to animals are enviable features for any AI system. Therefore, "biocontrol" [74] can be executed on different levels by a variety of algorithms. For instance, neural network models can exhibit types of neuron behavior found in some insects as well as those witnessed in humans. Observed techniques of voluntary movement as well as reflex responses to potentially harmful stimuli can also be elicited. Furthermore, appearance of higher level "intelligence" can be imputed to automata by furnishing them with biologically inspired motivations [14].

A given system may express varying degrees or combinations of these biological congruences. For instance, an *anthrobot* may achieve quite a plausible translation of human form and movement, but it

may not internally support the complex levels of perception, motor-coordination, and learning akin to real nervous structures. Along these lines, we have made similar choices as to what features of the human hand and biological control to include in the present study.

Physical Anatomic Consistency

Robot finger designs that purport anthropomorphism typically consist of 2–3 hinge-like joints that articulate the phalanges. In addition to the pitch enabled by a pivoting joint, the head knuckle, sometimes also provides yaw movement. However, as explained below in the examples of related work, the condyloid nature of the human metacarpal-phalangeal (MCP) joint (Figure 2.3) is often separated into two rotary joints. This has been known to complicate computer control of the mechanism because the extended axes of the joints cannot be easily coupled [92]. It is also interesting that in terms of whole hand designs, the use of five fingers is noted as being overly complex for most grasping and manipulation tasks. Crowder [35] for one, touts the general-purpose ability of three fingered configurations. In fact, the evolutionary catalyst for a five-fingered hand is still not well-defined and may be more physically related to our early water based ancestry than it is functionally inspired.

The underlying structure and articulation of the robot built for this thesis is modelled after the bones and joints of the human index finger (see *Chapter 2*). However, this version of the finger does not convey a third DOF in the MCP joint. This omission was made to allow for higher tactile resolution due to simpler fiber-optic cable routing. We do not expect the addition of this DOF to be a difficult problem and have already investigated potentially viable solutions to its incorporation. It is important to point out that artificial joint technology cannot yet replicate the self-lubricating triumphs of physical joints which orchestrate sliding cartilage and synergistic tendon attachments within the confines of the skin. Experimentation with new elastomer composites and 3-D printing techniques may lead to developments in this area.

Another reason for keeping the size and shape of the robot anatomically consistent is to facilitate automatic grasp and sensible use of conventional tools designed for human finger placement. Built in great part by and for us, the world is full of objects and activities that conform to our natural mechanics— from the buttons on our shirts to the door handles on spacecraft. This holds true for many manipulator applications, especially in prosthesis and tele-manipulation where accuracy of a human hand model enables more intuitive control of the slave

hand. These circumstances suggest that adherence to human geometry is a worthwhile pursuit.

As described above in Section 1.1.1 in relation to human muscle, a useful appraisal of actuator specifications can be made by looking at natural systems. Our robot's actuation scheme does not attempt to mimic these capabilities, but to assume some of the pertinent characteristics of low-powered, compact force generation. Clearly rotational motors and cables do not liken the linear contractions of our muscles that drive our joints. Though it is possible to view cables as tendons, the analogy is not one meant to persist. The cable transmission scheme employed uses *N* independent actuators to control *N+1* DOF. This is obviously not the case in the tendon arrangement of the human finger. We have, in fact, done some research into the use of Shape Memory Alloys to effect biological kinds of movement, however we believe full exploitation of the technology is not yet viable in the macrorobotic arena [10]. It may also be advantageous to employ series elastic actuators [90] to this effect.

Touch Sensing

As there is yet no comprehensive sensing suite available that meets the requirements for robot manipulation, much of the knowledge is drawn from the properties of the human tactile system. This hierarchy of touch sensing provides useful indications of the parameters of our research, from the quantity of feedback it avails to the reliance on this information of manual performance and body concept.

However, the application of some tactile characteristics to our robot is as far as the anthropomorphism extends. The intent is only to extract information of similar content to that received by our tactile modalities, not to reproduce the natural mechanisms responsible for relaying tactile feedback. It is important to note, that we only implement a single type of tactile sensor in this work. Tactile sensitivity of the human hand, however, consists of various components, responsible for detecting different types of tactile stimuli. These mechanisms, both organic and artificial, are further discussed in *Chapter 4*; their putative involvement in cognitive development is addressed in *Chapter 5*.

Furthermore, we believe that our sense of touch is inevitably linked to human survival, at least through our formative infant years. This may be one reason that our tactile apparatus has evolved to be so multifaceted and distributed. (And a reason why it is nearly impossible to find documentation on people born without such a sense, but common to find examples of congenital deafness, blindness, etc.) Because devel-

opment of tactile sensing technology is such a challenge, most humanoid projects, let alone manipulator platforms, either do without the ability or de-emphasize it in relation to vision, audition, and proprioception. To us, this seems a misappropriation on the part of researchers out to specifically extrapolate human cognition to a robot and/or to define that cognition by trying to recreate it. Therefore, this work is motivated by both the desire to build a hand for dextrous manipulation as well as the desire to avail a practical taction technique to others who also wonder what makes us human.

Biological Control and Processing

Human infancy is a time of systematic neurological and physiological change. The neophyte, initially lacking sensory-guided coordination due to underdeveloped sensory and motor mechanisms, engages with the environment through motor reflexes and sensory-triggered motion. As the baby develops, its cognitive, sensory, and motor systems harmoniously mature in phases, with certain abilities present at different times. When scaffolded upon one another, these developmental stages coincide with an assortment of increasingly sophisticated interactions with the environment—from purely reflexive behavior to voluntary, sensory-negotiated control. Such time-varying behavior is speculated to help manage the acquisition of incrementally complex world representations, form categories and predictive models from sensorimotor experience, and structure learning about the self and one's external surroundings [31].

In particular, the human hand has been cited as playing a crucial role in the cognitive functions listed above [105]. It follows that the manual conduct of human infants is considered a vehicle for cognitive stimulation as well as refinement of sensorimotor activity [84, 98].

Our approach to anthropomorphic robot control emphasizes our belief in the importance of the timely sequence of sensorimotor morphogenesis. Therefore, this works starts at the beginning, approximating the most basic newborn hand functions thought to strategically introduce the child to the outside world. We implement a version of neonatal grasping modelled after the reflexes that dominate manual behavior during about the first three months of life. These grasps are described as being *isometric* functions, that is, they involve static constant force exertion by the finger segments without any motion [30]. The robot also demonstrates some self-protective pain reflexes. By converging upon a more developmental trajectory toward anthropomorphic observance, we hope to lay a foundation off of which one could

bootstrap more advanced learning. Therefore, beyond just the practical aspects of achieving a manipulator with integrated tactile sensing, our approach offers an opportunity to answer broader questions about artificial cognitive processes. Is it possible to simulate cognitive development starting with a minimal set of human sensorimotor abilities? If so, can we ascertain requisites for a humanoid learner? If not, what developmental variations *do* ensue and what initial conditions are we missing?

Our controller employs tactile feedback to estimate properties of the contact between the robot finger and an object, without using prespecified strategic motions or geometric models. It actively uses the results to grasp the object due to hard-wired sensory/motor association. Because we are studying one finger, the robot is only presented with objects of size and shape that allow for their retention and support by the three encompassing finger links. Prehensile contact is maintained until a "reflexive" command to release the object is received. Theories about the evolutionary motivation behind such reflexes and their role in cognitive development are further discussed in *Chapter 5*.

The approach is considered "top-down," focused on simulating psychologically plausible movement, not on modelling any of the hierarchical neural architecture involved. This approach is also said to adhere to principles of "synthetic psychology," in which an observer can ascribe a sort of human teleology to robotic behavior [99, 13]. For instance, our robot might be seen as wanting to hold something or feeling pain. Therefore, at this stage in the research, we do not undertake any biologically inspired techniques for auto-associating motor and sensory data or any strategies for learning about these associations. Nor do we implement any notably human pre-grasp hand shaping, manual exploration, or object classification. The fact that these voluntary tasks involve more DOF in multiple fingers and a palm obviously prevents us from doing them with a single digit. Another reason for postponing these actions, is that their implementation can be greatly simplified by integration of visual feedback [102], which we do not have.

1.2 Related Work

There have been a number of robotic hand implementations that subscribe to different levels of anthropomorphism. One of the challenges of this line of research is that too close an emulation of human anatomy often proves cumbersome while a severe divergence from it sacrifices dexterity. The selection of leading hand designs reported here (in rough

chronological order) is limited in scope, addressing mechanical architecture, not control or sensing schemes. While some of these hands did have some variant of a haptic system (i.e., tactile and/or kinesthetic instrumentation), the success of others was considerably limited by their lack of such feedback. Thus, researchers have since modified commercially available versions of some these original designs to incorporate more elaborate sensing techniques. General descriptions of tactile sensing devices applied to any of the following examples are reserved for *Chapter 4*.

Furthermore, because the project concentrates on a single digit, only the finger designs from the following examples of whole hands are emphasized. Thumb descriptions are excluded unless the thumb is identical, yet in opposition, to the other fingers. The list excludes single or two-fingered constructions because most were designed to function as grippers and would not integrate well into multi-digit configurations.

- **Belgrade/USC Hand (1969)** [104] The Belgrade/USC Hand has four fingers, each with three parallel axis joints and one DOF that allows for "synergistic flexion" of all joints in unison. This configuration decreases the dexterity of the hand. Pitch for each pair of adjacent fingers is driven by a single motor which actuates the pair's most proximal knuckles. A separate linkage system in each digit then transmits power to the more distal joints. Rocker arms in the palm of the hand allow for finger compliance about the yaw axis. This hand has no tactile sensors, but does incorporate twelve force sensors (two per digit, two on the palm) which logarithmically indicate the forces exerted on it.

- **The Stanford/JPL (Salisbury) Hand (1981)** [94, 95, 75, 85] This system connects four flexible Teflon-coated steel cables originating from a remotely situated DC servo motor assembly to the joints of each of its three 3-DOF fingers. Thus, the hand is said to adhere to the *N+1* tendon-drive configuration in which *N+1* cables and motors are required for *N* DOF. Each digit has a double-jointed head knuckle providing 90° of pitch and yaw and another more distal knuckle with a range of ±135°. Although the modularity of the fingers makes them simple to build, dexterity is sacrificed because the axes of the joints do not all intersect. Furthermore, the drive assembly is ungainly and the push/pull flexible cables are of limited reliability and power transmission capability. Cable tension-sensing mechanisms based on strain gauges ensure accurate control of forces at the fingers.

- **The Utah/MIT Dextrous Hand (1982)** [59] The 4-DOF digits of this hand outwardly parallel the structure of a human finger, although a non-anthropomorphic design of the head knuckle excludes circumduction. The inclusion of three fingers minimizes reliance on friction and adds redundant support to manipulation tasks. Each *N*-DOF finger is controlled by *2N* independent actuators and tension cables (i.e., a *2N* tendon-drive configuration). These tendons are part of a complex cable drive system propelled by 32 specially designed pneumatic glass cylinders and jet-pipe valves. Rotary Hall effect sensors mounted in each finger joint relay joint angle measurements. Although the fingers exhibit high dynamic performance, with fingertip force exertion of 7 lb and frequency components exceeding 20 Hz, their implementation is cumbersome. The drive system degrades finger control and kinematics due to the unreliability and compliance of long cables, elaborate pulley systems required for friction management, and a large motor apparatus.

- **The Hitachi Robot Hand (1984)** [78] The Hitachi Robot Hand achieves fluid joint movement and compact design by utilizing SMA actuation. Each of the three fingers has four joints each of which in turn is driven by actuators built into the forearm. The actuators bend the digit by pulling a drive wire and relax the digit by shrinking back against the force of a spring set into each joint. Therefore, these SMA driven mechanisms can be seen as active muscle/tendon systems, whose attachments and contractile, load-carrying abilities directly initiate the motion of the whole apparatus. Furthermore, these devices are capable of manipulating a 2 kg object due to the parallel incorporation 12 very thin SMA wires per finger. The fingers are compact, have a good power/weight ratio, and are capable of high speeds and load capacities. However, there is performance degradation of the SMA after many cycles, making the system prone to failure.

- **The Matsuoka Hand (1995)** [76] This is the first anthropomorphic scale hand developed for Cog, the humanoid platform of the MIT Artificial Intelligence Lab. Each finger comprises two phalanges and two coupled joints. These joints are controlled by a tendon cable/pulley/motor system that imparts two apparent (through one mechanical) DOF to the device and is capable of generating a torque equivalent to a 0.5 lb fingertip exertion. The platform is self-contained although the finger motors lend much weight and size to the corresponding hand. Reduced strength

and precision of these fingers is acceptable because Matsuoka aims at simulating infant level learning skills for manipulative movements.

- **The Robonaut Hand (1999)** [73, 3] This robotic hand, designed to match the size, kinematics, and strength of an astronaut's gloved hand, is broken down into two sections. The dextrous manipulation work set includes two 3-DOF fingers; the stable grasping set includes two 1-DOF fingers. A stainless steel flexshaft coupled to a brushless DC motor housed in the forearm transmits power to each of the fingers. The base joints of the *dextrous* fingers allow for $\pm 25^\circ$ yaw and 100° pitch; the second and third joints are directly linked to close with equal angles. The *grasping* fingers have three pitch joints that close with approximately equal angles over a 90° range. Due to the complex geometry of the hand, many of its parts were cast in aluminum directly from stereolithography models. Absolute position sensors embedded into each joint in the hand, incremental encoders on the motors, load cell assemblies, and tactile sensors provide position and force feedback for control.

- **DLR (2000)** [55, 23] The DLR (Deutches Zentrum fü Luft- und Raumfahrt) Hand is a multisensory, articulated hand with four fingers typically controlled through a data glove. Specially designed linear actuators integrated into either the palm or directly into the proximal finger links manipulate the joints of the fingers. Each finger has a 2-DOF base joint capable of $\pm 45^\circ$ of flexion and $\pm 30^\circ$ of abduction/adduction, a 1-DOF knuckle capable of flexing 115°, and a distal joint capable of flexing 110°. The distal joint is driven passively due to interjoint coupling. Position, force, and stiffness control are carried out by the use of strain gauge based torque sensors, optical joint position sensors, and tactile foils.

The reader is referred to [50, 39, 22, 78, 101, 43, 4, 24] for other examples and surveys along this line of research.

1.3 Organization of Thesis

This thesis is broken up into parts according to the main steps taken in the realization of the robot: physical construction, actuation design, sensor design, and control. Granted, these stages are very much interdependent—with the control finally integrating all the other modules. However, in this text, they are considered separately in order

to show how each one contributes to the project and affects the intended goal of a contact control-based robot finger. The next four chapters detail the design processes, materials, technologies, and algorithms involved in implementing the robot along with descriptions of the corresponding biological identities.

- *Chapter 2* outlines the physical architecture of the robot. As a reference for the reader, the chapter opens with a summary of the terminology used to describe the structures and motions of the human finger. These terms are then used throughout this paper in reference to the artificial finger. The chapter proceeds with a condensed introduction to the bones and joints of the human finger. It also covers the mechanical design and fabrication processes employed in building the robot, from the initial computer-aided design (CAD) tools to the final stereolithographed joint constructs.

- *Chapter 3* opens with an outline of the human muscles and tendons involved in those finger movements that are relevant to this work. These biological entities are very different from the actuators of the robot. Thus their presentation is meant to emphasize this contrast, not to force anatomical nomenclature onto artificial mechanisms. The hardware components and function of the robot's actuation system are presented.

- *Chapter 4* offers a brief introduction to artificial haptics, emphasizing the impact of tactile sensation on end-effectors. We survey the most widely used pressure sensor technologies and describe the fabrication, operation, and evaluation of the sensor used on the robot finger. As is the practice, descriptions of human exteroception and skin are given. A short explanation of fiber-optic technology is also included to facilitate understanding of the tactile sensor application used in this research.

- *Chapter 5* outlines a simple software example of motor control integrated with the tactile feedback to beget reflexive behavior. Experiments with tactually-based robot grasping and their results are given. Because we do not approximate a model of anthropomorphic sensorimotor control, the human sensorimotor system is addressed in terms of the biological inception of infant dexterity. This development is used as a springboard for the integrated actuation-sensation system of the robot finger.

- *Chapter 6* poses suggestions and goals for future work. Those suggestions mentioned previously in their appropriate contexts are not reiterated.

Chapter 2

The Embodied Robot

A thorough description of the anatomy of the human hand, or even a single digit, would be prohibitive here, as would be a survey of the numerous, and often conflicting, functional analyzes and kinematic models that have been proposed to that end [21, 11, 19, 7, 91]. This chapter adopts a simplified representation of the hand as a linkage system of intercalated bony segments [7]. It emphasizes the bones, articulations, and some of the ligaments involved in flexion and extension of the index finger—which serves as the template for the robot finger. Those internal features implicated in actuation (e.g., tendons, muscles, and their artificial counterparts) are described in *Chapter 3*.

Figures 2.1 and 2.2 provide a reference for anatomic orientation, surface, and finger movement terminology. As the pictures illustrate, flexion is defined as the bending of, or decrease in angle between, articulated body parts. Extension is the opposite of flexion, resulting in a straightening of anatomic links. In regard to fingers, adduction and abduction are defined, respectively, as motion away from or toward the midline of the hand, i.e., the vertical axis of the middle finger. (However, the robot is not capable of these two motions.)

The following notes should also clarify some of the vocabulary used throughout this text:

- Motion generated solely by internal musculature is referred to as "active" movement, while that induced by external forces is called "passive." For instance, one can passively extend her MCP joint beyond its limit of active extension by pushing a straightened finger against a surface while lifting her palm (see Figure 2.2*c*).

- The terms "proximal" and "distal" are anatomical descriptors

meaning "closer to" and "farther from the central body," respectively. Thus, the distal phalanx is at the tip of the finger; the proximal phalanx is the finger bone closest to the palm.

- Ranges of flexion and extension for finger joints are defined relative to the hand's frontal plane which is defined as being parallel to the flat hand with its fingers extended. Sometimes this straightened finger pose happens to be one of maximum extension, as it is for the proximal interphalangeal (PIP) joint (see Figure 2.3). Therefore, though a joint may be defined as having a significant degree of flexion (and can therefore extend back through that joint), its range of active extension may be nil. These characteristic joint range values are not to be confused with general joint movement, which is a measure of the angle formed by the long axes of two adjoining body segments.
- Though it is basically similar in structure, the thumb is not considered herein. Any mention of fingers or phalanges of the hand refers only to the four longer digits.
- The terms "phalanx" and "phalange" are anatomically used in reference to the whole finger as well as to the individual finger bones. We maintain the latter definition throughout the text.

2.1 The Anatomic Frame: Finger Bones and Articulations

An understanding of the skeletal and joint structures of the human hand is a starting point for the development of a mechanical general-purpose manipulator. Though there is still much to be known about the hand's functional parameters, the topography of its bones has long been determined. Figure 2.3 shows the bones and joints of a human digit from two different perspectives. Each of the four fingers comprises 3 of the 27 bones of the human hand: the proximal, middle, and distal phalanges, extending from the palm outward. The first two of these segments are considered long bones, having tapered shafts that are concave in front, convex in back, and flat from side to side. The extremities of these shafts are referred to as heads and bases. The distal, or ungual, phalanx is small and convex on its dorsal side. Its flat palmar surface presents a roughened horseshoe elevation which supports the pulp of the fingertip [51]. Joint angulation is expressed by movement of these bones along the articulated surfaces of each other.

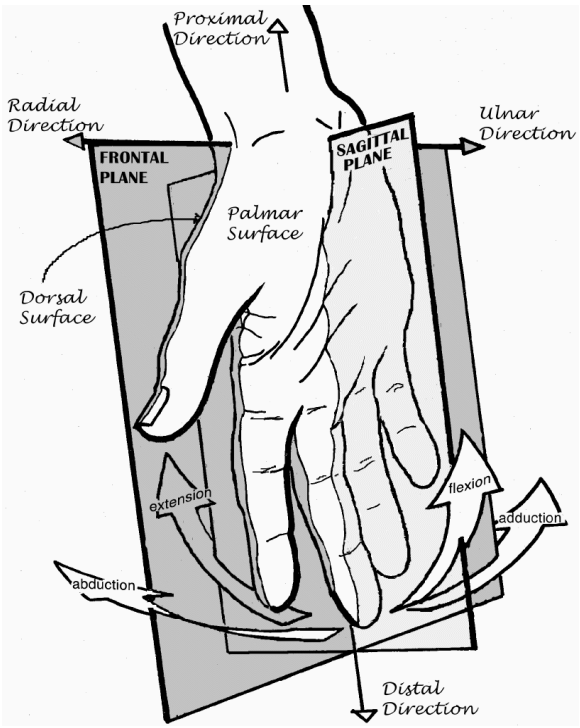

Figure 2.1: Orientation, surface, and finger motion terminology. Abduction/adduction arrows correspond to index finger motion. Adapted from [64].

This movement of the bone segments is prescribed by muscles, tendons, ligaments, synovial joint capsules, and other bony features which restrain the joints from having six DOF [91]. Fibro-cartilaginous plates that slide along the surfaces of adjacent heads and bases are critical to joint operation. Such structures are not described in detail here, as there are no direct substitutions for them in the robot.

In the finger, the joint closest to the palm, connecting the head of the metacarpal and the base of the proximal bone, is called the metacarpal-phalangeal (MCP) joint. It is of a 2-DOF condyloid type, in which an ovoid head is received into an elliptical cavity [51]. Treated ideally as a saddle or universal joint, it allows flexion/extension, or pitch, in the sagittal plane and adduction/abduction, or yaw, in the frontal plane. For the index finger, the MCP joint's range of flexion is nearly 90° from the neutral position when measured with respect to

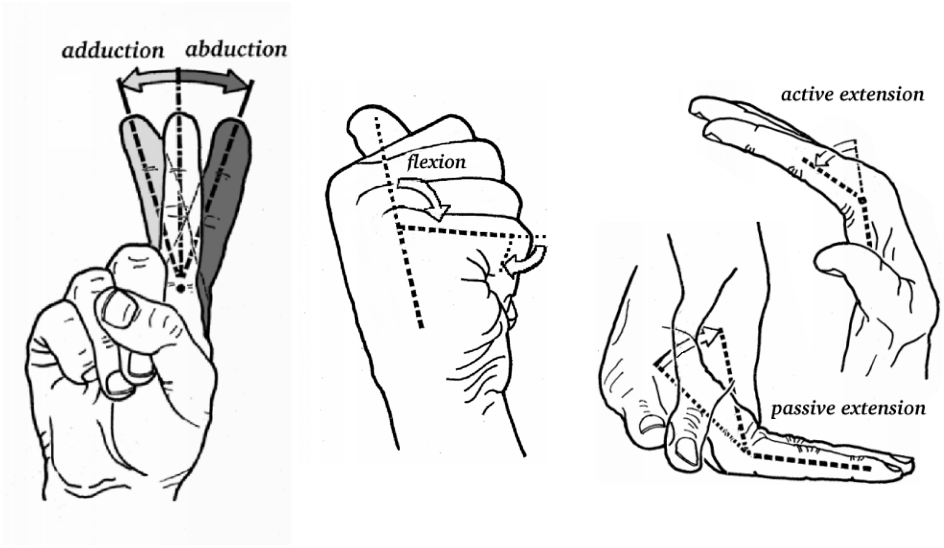

(a) (b) (c)

Figure 2.2: (a)Adduction/abduction, (b) flexion, and (c) active/passive extension of human fingers. Adapted from [64] without permission.

the metacarpals. This range increases progressively to about 120° for the little finger. The joint's range of active extension can reach 30°–40° and its range of passive extension can reach up to 90°. Because of its shape, the MCP joint of the index finger is also capable of 30° of adduction and abduction, the greatest of all the fingers. This motion is usually only possible when the joint is extended because of tension in the collateral ligaments. These ligaments are responsible for holding the articular surfaces together and partially confining their movements.

The PIP and distal interphalangeal (DIP) joints adjoin the proximal phalanx to the base of the middle phalanx, and the head of the middle phalanx to the base of the distal phalanx, respectively. Often characterized as hinge joints, they each have only one DOF: flexion/extension in the sagittal plane. For the index finger, the PIP joint flexes slightly beyond 90°, forming an acute angle between the proximal and middle bones. It does not demonstrate any active or passive extension. The range of flexion for the DIP joint in the index finger is slightly less than 90°. Its range of active extension can be up to 5°, while that of passive extension is about 30°. Articulation of theses two joints is coupled through flexor and extensor tendon dynamics (see *Chapter 3*).

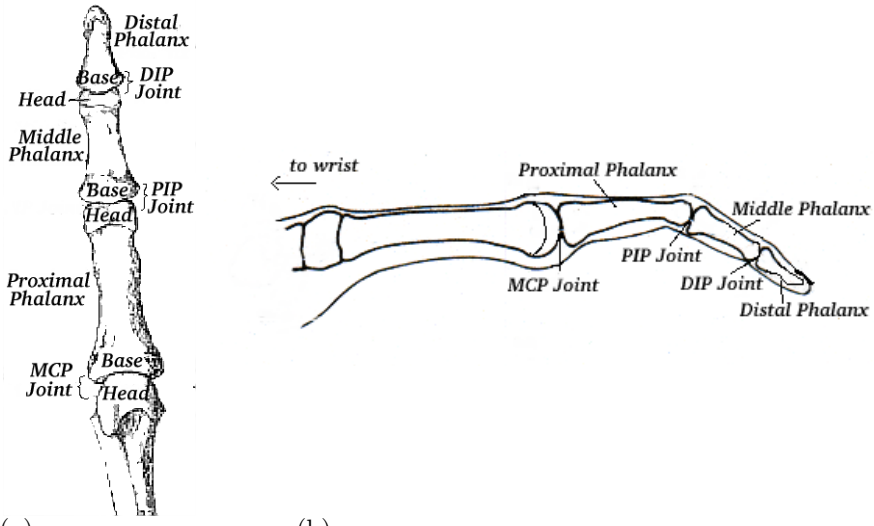

Figure 2.3: (a) Palmar and (b) lateral views of the bones and joints of the human index finger.

2.2 The Robot Analogue: Skeletal Structure

The components of the robot are referred to throughout this text by the names of the corresponding anatomical parts.

The 2-DOF robot skeleton, depicted in Figure 2.4, is modelled after the human index finger. One reason for choosing the index finger as a template, is due its adjacency with the thumb. This configuration imparts the index with the greatest mobility of the four fingers and the most dynamic infrastructure. Furthermore, the fact that the index finger flexes strictly in the sagittal plane, unlike the other obliquely flexing three fingers, makes the articulation design easier (Figure 2.5). For example, in integrating it into a hand, copies of the finger could be placed at progressive angles on a palm structure or slight modifications could be made to the robot's link sizes and joint limits to more accurately model the other digits.

Special care was taken in the design of the linkages to replicate the basic geometry of the corresponding human finger bones. This was for functional purposes and to give the artificial finger an appropriate aesthetic when covered by the tactile skin. The robot, like its

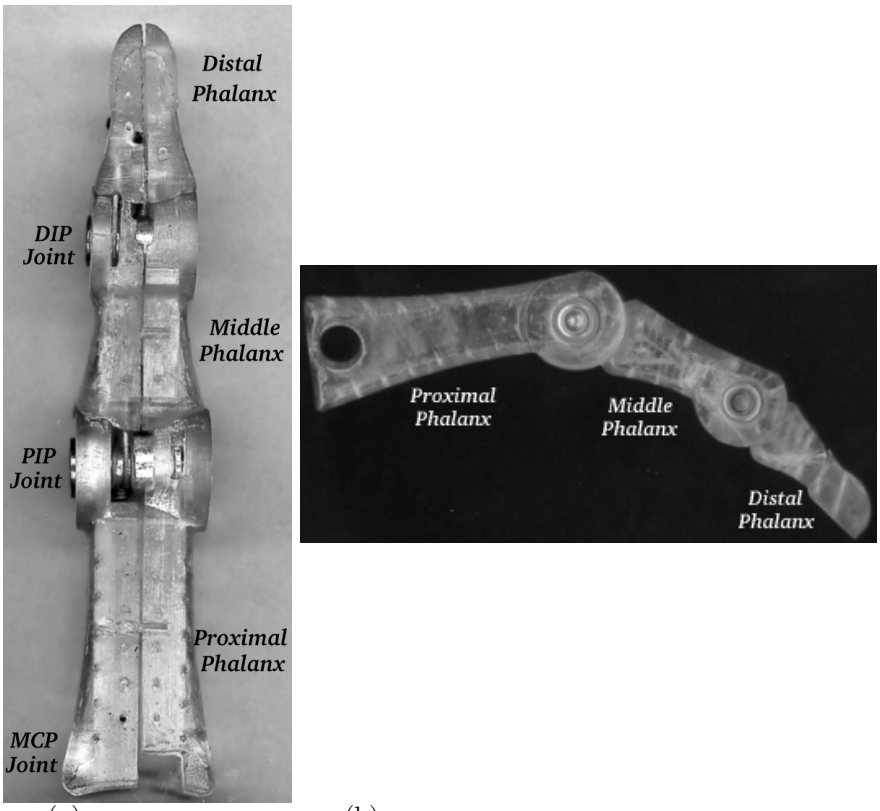

(a) (b)

Figure 2.4: (a) Palmar and (b) lateral views of the bones and joints of the robot finger. Tactile sensors and actuating tendons not included.

human counterpart, consists of three segments: proximal, middle, and distal. Their link lengths (4.70, 2.82, and 2.13 cm, respectively) and widths are extrapolated from external anthropometric hand data for a 50th percentile female [9] and from the author's finger dimensions. Some size adaptations were made, however, to allow for incorporation of bearings and mechanical stops at the joints. In future versions of the robot, we may investigate other techniques for modelling finger link lengths, such as approximation to the Fibonacci sequence [72] and proportion to joint center position [20, 109]. Though there has been considerable data published on bone lengths and hand measurements, it lacks valuable kinematic content [87, 44, 45, 7]. This is because bone

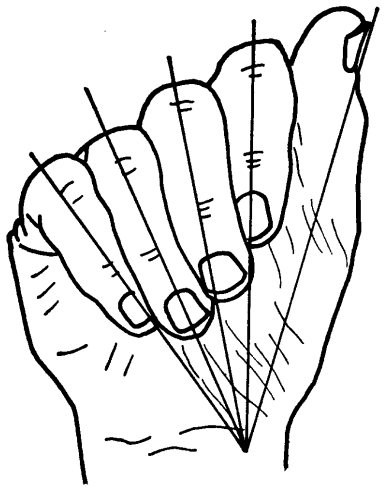

Figure 2.5: The axis of the bent index finger is vertical while the axes of the other fingers become more oblique the farther they are from the index. [64]

link lengths are not equal to the effective link lengths which define the moment arms for joint torque generation. Therefore, it is necessary to determine the locations of the centers of joint rotation and axis directions for flexion and extension. Buchholz et al. [20] corroborates the approximation of this axis at the centers of curvature of the bone heads proximal to both the PIP and the DIP joints (see Figure 2.6). Though their investigation of kinematic hand anthropometry proposes this as an adequate estimate for use in many biomechanical models, we extend this applicability to robotic manipulators. Therefore, we have constructed the artificial finger joints as hinge joints. This is not only a popular mechanical approximation; the convention is also commonly used in hand modelling, for it has been shown that inter-joint distances remain fairly constant during flexion and extension [29].

The hinge axes for the robot's PIP and DIP joints are fixed through the centers of curvature of the heads of the proximal and middle phalanges, respectively (see Section 2.2.1 for how this is done). These heads are pulley-shaped like their anatomic counterparts, therefore enabling the same joint flexions and extensions in the sagittal plane about single transverse axes. The shape of the base of the immediately distal link fits like a puzzle piece (i.e., a curved convex surface) into this head, approximating the two shallow facets and median ridge on human pha-

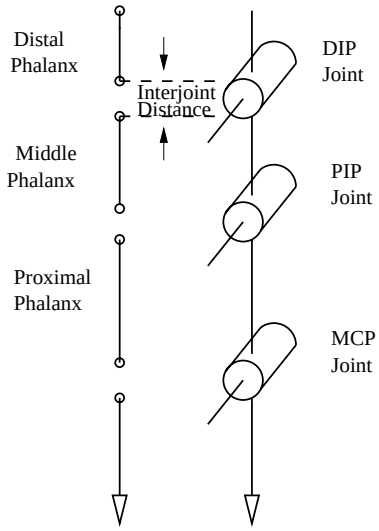

Figure 2.6: Articulated finger links modelled with mechanical hinges. Concept from [91].

langes. The flat lateral sides of the head pulley act to restrict any yaw DOF of the joint. These articulating surfaces slide directly against each other, unlike human joints in the which bone contacts are separated by cartilage that is lubricated with synovial fluid.

The maximum relative motions of these joints are kinematically similar to those of the human hand. The PIP joint can undergo 100° of flexion, while the DIP joint can flex through an angle of 80°. Neither joint is capable of any active extension, and any passive extension due to cable laxity is neither intentional nor optimal. These ranges are checked by physical stops directly built into the robot's bone segments, as opposed to by restraining anterior and lateral ligaments (see Section 2.2.1). Furthermore, the DIP joint angle depends on the PIP joint angle due to bidirectional cable coupling. In the human hand, these joints are also coordinated, though their coupling is due to tendon interplay, not to direct connection.

The range of flexion of the robotic MCP joint is 90°; its range of extension is 40°. Unlike that of the other two joints, this angulation is delimited through motor control, not physical stops. Also, the axis of rotation for the MCP joint lies in the base of the proximal link in order to conserve space and because we don't implement any metacarpal bone

in which it would actually reside. The whole robotic finger is connected to a portable Plexiglas base by a steel dowel pin that determines this axis (see *Chapter 3*). The base also serves as a housing for the motors and is of a "hand-size" proportional to the robot finger. It can be turned upside-down to allow for wrist-like reorientation of the finger.

2.2.1 Fabrication Processes

The robot skeleton was designed in SolidWorks, a CAD software package (see Figure 2.7). These linkages were then built using a rapid prototyping (RP) technique called stereolithography, on a 3D Systems SLA250-40 machine (referred to as a stereolithograph apparatus (SLA)) at Draper Laboratories. Like all other RP technologies, SL is a manufacturing process by which physical 3-D models are automatically rendered from CAD data. This is achieved by laser tracing successive cross-sectional slices of an object in an epoxy-based UV-curable photopolymer. Because this is an "additive" process, as opposed to other machining methods which remove, or subtract, material in order to fashion a part, pieces with complex contours and internal voids can be fabricated.

This capability for generating hollow, biologically shaped objects was the main motivation for choosing SL, fueled by the desire to create bone-shaped structures that would accommodate cable and sensor routing within. (The three links of the robot finger were actually made in halves in order to facilitate installation of the actuator transmissions and optical fibers of the tactile sensor.) Because the SL process allows for fast turnaround from design submission to product visualization (typically about 4 hours for the aforementioned parts), expeditious design enhancements and error elimination was made possible through trial and error experimentation. Multiple copies of parts can also be fabricated in one build cycle. This is a compelling feature to any robot experimenter, as it is good practice to have spares made in case of unforeseen failures. All of these facets can amount to substantial cost savings in the overall production life of a research system [8, 106].

As this version of the finger was manufactured on a small scale and mostly intended as a tactile sensor test bed, it was possible to use the resulting plastic prototypes in the actual robot. However, the plastic is really too brittle to support the higher loads and grip forces sustained by a fully functional artificial hand in a realistic workspace. Eventually the fingers will have to made out of one of the more robust, non-polymeric materials or metals that are now being introduced into RP techniques. SL is also not the optimal option for mass production

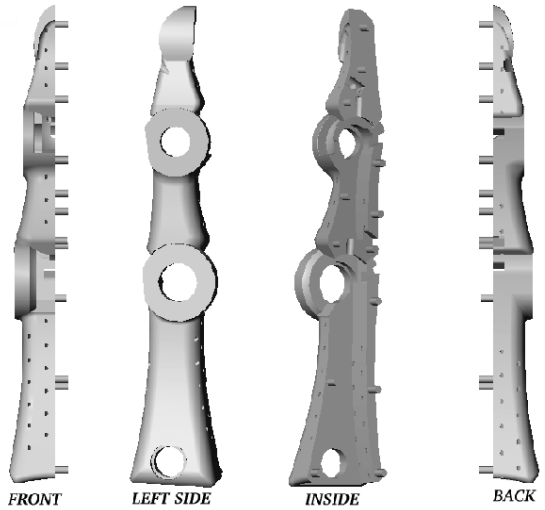

Figure 2.7: Frontal, lateral, internal, and dorsal views of a SolidWorks assembly of the left half of each robot finger link. The tunnels passing from the front to the back of surfaces are guides for the fiber-optic cables comprising the tactile sensors. Other crevices are steel cable routes, cable termination compartments, and receptors into which the right halves fit.

applications. In these cases, it is more efficient to use SL to make a mold which can in turn be used for casting replicas. We hope to use this procedure to obtain aluminum parts for future robotic fingers.

The use of SL was further motivated by the currently limited application of rapid prototyping to robot design. Although it has been used at the MIT AI Lab for aesthetic purposes (e.g., as a face shell for a binocular vision system [41]) and incorporated elsewhere into other functional devices [67, 107], there has not been much evidence of biologically inspired part reproduction. One other interesting employment of SL that has begun to receive particular attention from robot engineers is the fabrication of multi-DOF systems that do not require assembly. The SLA can achieve this by constructing the specialized housings and the embedded, moving components of prismatic, universal, revolute, and spherical joints all at once [2]. Along these lines, RP techniques may someday be able to integrate different materials into a single build.

This would make way for the inclusion of flexible elastomers between hard surfaces, simulating the soft cartilage in human joints.

We did not exploit this capability for pre-assembled joint construction in the current version of the robotic finger. In order to augment the structural strength of the assembly, the joint pulleys of the robot were, instead, machined out of aluminum and then pressed onto 0.125 inch diameter steel dowel pins (see Figure 2.8). These steel pins were then horizontally mounted into miniature bearings embedded into both halves of the SL'd linkages. Each of the three dowels thus forms one of the axes about which a finger link rotates. The axis pin of the DIP joint internally connects the centers of the heads of the two halves of the middle phalanx. The axis of the PIP joint (about which the middle phalanx rotates) does the same for the halves of the proximal phalanx. The MCP joint axis is much longer than the other two axes. It extends through the base of the proximal phalanx to connect the finger to the motor housing.

The joint axis for both the distal and middle phalanges lies in the head of the previous link. Therefore, each of these phalanges must be connected to its corresponding joint mechanism by a small vertical dowel pin (see Figure 2.8*b*) that extends out of the previous link's head. Upon construction, two semicircular holes in the bottoms of the halves of both the distal and middle links close tightly around the dowel. This is how the adjacent bones are joined together.

In contrast to the metal joint mechanisms, the joint stops *were* designed directly into the SL'd pieces. Bevels in the heads and bases of adjoining segments align at the joint limits to keep the links from overextending or flexing beyond their intended angles. *Chapter 3* provides more details about the joints of the robot.

SL is a versatile complement to traditional machining processes and robot fabrication methods. Yet, it is important to note that extra pains must be taken during the design phase in order to prepare for some of the limitations of the technique. In particular, we had to incorporate extra room for through and press-fit holes due to discrepancies between the CAD precision and the SLA tolerances. Similar allowances had to be made for clearances between moving parts. Also, step-like profiles on rounded features, due to the linear approximation of continuous curves that the SLA software utilizes, had to be smoothed over with metal files.

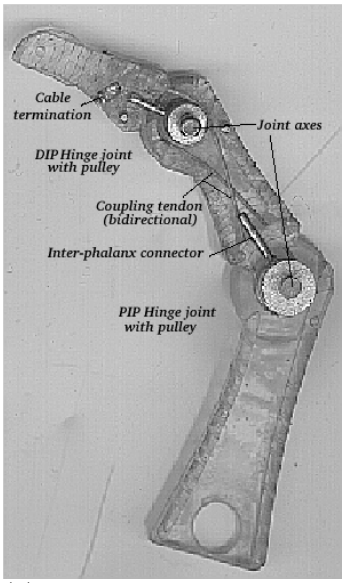

(a)

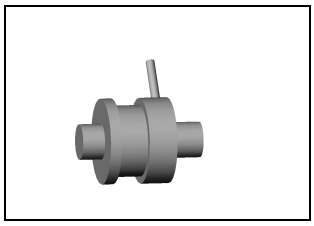

(b)

Figure 2.8: (a) Internal view of the joints embedded into the finger and (b) SolidWorks sketch of the DIP joint pulley.

Chapter 3

Actuation Hardware

In presenting an anthropomorphic approach to the construction of a robot, there is an urge to describe artificial mechanisms in terms of similarly functioning biological entities. Though this kind of comparison can be useful, there is a point at which assigning anatomic nomenclature to the robotic parts can be more misleading than informative. This is the case with regard to the actuation system of our robot. As previously mentioned, the magnitudes of tendon and joint forces in the human hand, the way in which they are transmitted, and their correspondences with one another are still under-defined for many manual functions.

In Section 3.1, we introduce some of the biological units responsible for actuation the human index finger. This summary is meant to broach a few limitations of our anthropomorphic approach. The initial intent was to discuss only the primary muscles involved in the human finger motions that our robot can also achieve—namely flexion, extension, and isometric poses in the sagittal plane. However, there is rarely a one-to-one correspondence between a muscle or tendon and a joint action, especially in the polyarticular hand. Muscle coordination in the hand is known to be mathematically redundant, particularly when the system is performing below its maximal physiological strength. So, though each muscle may be said to have a primary function, the motion of the finger is ultimately determined by the combined influence of many muscles' motion potentials. Furthermore, there are many different muscle combinations that can provide the same required strength.

Although some preferable muscle force distribution patterns may exist, it is not possible to uniquely determine which of these combinations achieves a particular static force; the central nervous system does

not seem to employ only those muscles which are "mechanically" necessary for the task. Instead, its "objective" may be to minimize overall fatigue or conserve the system's total output energy. This is especially true for functions pertaining to this research i.e., in which the hand or finger must maintain a particular isometric pose for an extended period of time. Under such circumstances, all muscles suitably situated to generate the intended joint torques may contribute varying, yet compensatory magnitudes of force. These muscle forces may participate as moderators, antagonists/synergists, direct actuators, and even passive restrainers.

In light of these observations, our goal is not to misrepresent the limited tendons and motors used in the robot finger as having biological analogies, but to accurately portray their shortcomings. The following section provides only very general explanations of index finger tendon/muscle functions in order to point out an important departure from anthropomorphic consistency. The differences will hopefully delineate some of the issues to be considered when implementing more versatile actuation schemes.

3.1 The Anatomic Actuators: Human Hand Muscles and Tendons

Human fingers are actuated by extrinsic muscles originating in the forearm and less powerful, intrinsic muscles located distal to the wrist. The former generate the primary forces for isometric poses, while the latter provide for delicate maneuverability and stabilizations [30].

Connective tissues (collagen) which bind the parallel fibers that make up skeletal muscles join together at the ends of a muscle to form tendons. For the hand, these elastic tendons terminate on the finger bones. In the case of the extrinsic muscles, the tendons extend from remotely located muscles, spanning over multiple joints in the arm and the hand. They are tethered to intermediate bones by fibrous tunnels which allow the tendons to maintain their relative positions to the phalanges instead of assuming straight paths during flexion. Synovial sheaths are responsible for the smooth gliding of the tendons within the fibro-osseus tunnels. (We do not describe these features in detail because they are not simulated in the robot finger. The cable tendons in the robot traverse the hollow insides of the bone structures instead of following the surfaces of the bones. Thus, they are surrounded by air and protected from external impacts that might change their lengths.)

Experimental studies on normal and disabled hands demonstrate

that it is the arrangement and properties of their connecting tendons that primarily determine the range of motion of human fingers [11]. Due to tendon connections, the linear forces generated by bundles of muscle fibers are translated into torques about the knuckles. If this torque exceeds opposing torques from antagonistic muscles or external loads, then the corresponding finger bone rotates about the joint.

Because muscles provide power only during contraction, complementarily oriented muscles must issue tendons to the phalanges: flexors and extensors (see Figure 3.1). (Note, however, that besides providing flexion and extension, most tendons and intrinsic hand muscles also generate components of force producing rotation or deviation.) Control of the finger is the result of these and other muscles acting together on different sides of the rotational joint axes. The redundancy of the tendinous system enables antagonistically and synergistically contracting muscles to optimally tune the stiffness of articular joints for different tasks.

In contrast, actuation of any of the robot's joints involves only one actuator connected to a bidirectional tendon that at a single instance acts as either a flexor or an extensor. The torque at a joint is the result of only unidirectional contributions. Therefore, there is no way to regulate joint impedance independently of the joint's velocity or of the net joint torque induced by the motor. Furthermore, the steel tendons do not induce any *functional* forces other than those around their designated axes of rotation. (Joint coupling induced by cable friction is described below, but is not considered functional.)

The digital flexors of human fingers, whose fleshy bellies lie in the anterior forearm, are more powerful and less compact than the extensors, which originate in the posterior compartment of the forearm. This is evidenced by the slight flexion of the fingers when the hand is in its natural position, that is, when its muscles and joints are all in equilibrium.

More specifically, the flexor digitorum profundus (FDP) and the flexor digitorum sublimis (FDS) are thought to be responsible for much of the flexion of, respectively, the DIP and PIP joints of the index finger. Flexion of the DIP joint is shortly followed by flexion of the PIP joint, as there is no extensor to antagonize that action in the joint. Conversely, after the FDS has contracted to bend the middle phalanx, the FDP flexes the distal one. The result of these functions is an apparent coupling of the two joints.

The DIP and PIP joints are coupled in the robot by a single bidirectional tendon which terminates at both ends in the distal finger link and is intermediately routed around a pulley fixed to the rotational

axis of the PIP joint. Since only the PIP, not the DIP, joint has a dedicated motor, rotation at the DIP joint is completely dictated by rotation at the PIP joint and the two joints can never move independently. In contrast, some people are capable of decoupling these joints due to variations in tendon elasticity.

The extensor digitorum communis (EDC) and the extensor indicis propius (EI) enable much of the extension of the index finger. The EDC is named for the fact that the same muscle belly sprouts a separate tendon to each of the four fingers. Thus all the fingers have the same actuator in common. The tendon of the EI, however, issues solely to the index, allowing the finger to be extended singly.

These anatomical extensors act on all three finger joints. For instance, Figure 3.1*a* shows how, at the MCP joint, the deep surface of the EDC tendon separates to attach to the base of the proximal phalanx. The main fibers of the tendon then continue down the finger, merging with the EI, and splitting into three parts: the center part inserts as the *median band* into the base of the middle phalanx; the two outside parts form *lateral bands* that extend the length of the middle phalanx and finally terminate as one on the base of the distal phalanx. Thus, though the EDC essentially functions as an extensor of the MCP joint, it can also act on the PIP and DIP joints. Clearly such poly-articular arrangements are very different from those of the robot's tendons. In fact, frictional byproducts of idle pulleys which cause a dedicated tendon to induce motion at secondary joint only serve to complicate control issues. These are undesirable consequences.

The anterior interossei (AI), posterior interossei (PI), and the lumbrical (L) muscles are all intrinsic to the hand. Their tendons make various lateral attachments to the finger bones as well as blend with other tendinous structures. Both sets of muscles contribute to the degree of stabilization and sequence of joint flexion and extension in the index finger. These muscles also play dominant roles in adduction and abduction of the MCP joint. The robot finger can't perform adduction/abduction because its MCP joint is a hinge joint and therefore does not allow any ulnar or radial movement.

When joint motion is resisted, the above tendon/muscle systems allow for the hand to exhibit functional strength through a variety of isometric grips (Figure 3.2). These hand formations have been widely classified according to both anatomical and functional metrics [96, 103, 77, 48, 37]. However, Napier's [79] classification of grips into precision pinches and power grasps is the most widely accepted throughout the fields of biomechanics, medicine, and robotics.

For this research we are interested in a variation of the power grasp.

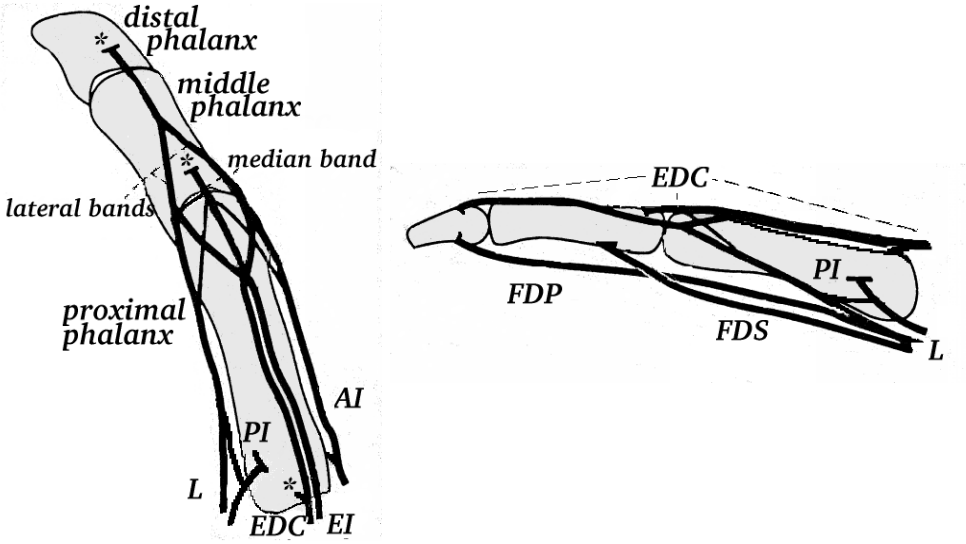

(a) (b)

Figure 3.1: (a) Simplified sketches of major tendons of the index finger. Asterisks show the tripartite insertions of the EDC into the proximal, middle, and distal phalanges. Note tendons often merge together, bifurcate, and change orientations relative to the bones. (b) The radial view also includes the primary flexors. Graphics adapted from [16].

In general, such a grasp is defined as "a forceful act performed with the finger flexed at all three joints so that the object is held between the fingers and palm, with the thumb acting as an additional stabilizing element" [30]. The grasp provides stability and security at the expense of the object maneuverability allowed by precision pinches. Studies [42] have shown that keeping a hammer handle from slipping out of the palm requires a power grasp of approximately 5 lb/in^2. (If touch sensation is impaired, then strength has to be increased to provide greater sensory feedback.)

After pre-shaping the hand (pre-grasp phase), voluntary grasps are normally carried out by placing the palm over an object, flexing the MCP and then the PIP and DIP around it, and then setting the pose to restrain the object (static grasp phase). Chao et al. [28] has experimentally determined that six phalangeal force distribution patterns are possible for grasps (e.g., the distal phalanx provides the greatest force followed by the proximal and middle phalanges.) These forces were assumed to apply at the middle of each phalanx. As described

in *Chapter 5*, this assumption is also exploited in the control of the robot finger grasping. (Wrist flexion/extension also plays a role in pre-shaping and fixing the grasp.)

This research primarily concerns tactile sensation on a single finger. Therefore this version of the robot cannot perform the canonical power grasps described above for there is no incarnation of a thumb or a palm. Instead, a grasped object must be held within the envelope of the three flexed finger segments. This is most akin to the hook grip. Though very useful to primates swinging from tree branches, this grasp is only employed by humans when, for instance, holding a briefcase handle.

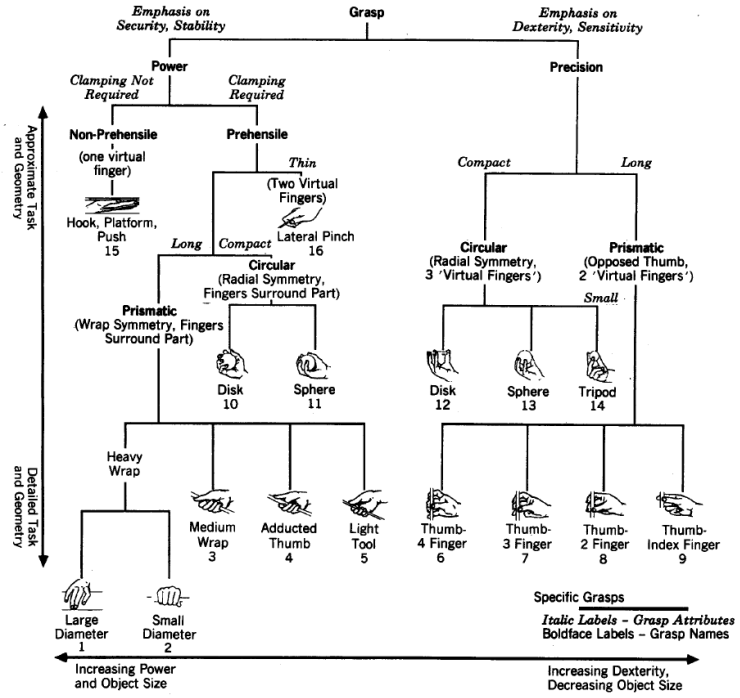

Figure 3.2: Partial taxonomy of human hand grasps. From [97] without permission.

Overall, the durability, versatility, and effectiveness of biological muscles are distant features of engineered actuators.

3.2 The Robot Analogue: Motor/Cable Transmission System

The issues of actuation and power transmission are of paramount importance in the design of multi-DOF manipulators. As Crowder [35] has reported, the most common implementations of power transmission in hands are flexible tendons and solid links.

We chose to use a cable drive system due to limited space inside the hollowed finger links. Tendon transmissions permit the actuators to be placed remotely from the joint axes, decreasing the moving mass of the articulated robot and therefore increasing the payload that the robot can sustain. This type of transmission also relaxes the constraints on the weight and size of the actuators that can be used, allowing power output specifications to take priority over mechanical dimensions. Such considerations would be even more crucial in a larger end-effector at the end of an robotic arm.

Furthermore, the cable system allows for easy modification of the motion of the fingers, as the pulleys, whose diameters prescribe the torque reduction ratios of the joints, can be simply replaced and the cable system re-tensioned. Despite these advantages, cabling in such restricted cavities is still fairly unwieldy. As a flexible cable can only be used to pull, a bidirectional cable system was required to achieve control of both flexion and extension of a joint. Much design effort was expended in ensuring that the consequently parallel tendons would not rub against each other or any of the sensor components. We intend to investigate other materials and implementations for actuation in future versions of the robot.

The actuation set-up for the robot is sketched in Figure 3.3. Two identical motors, one controlling the MCP and one controlling the PIP joint, induce motion in the finger. The motors are installed directly below the base link in a proportionally palm-sized Plexiglas box. Power is transmitted from these actuators to the robot's joints via 0.6 mm (.024 in) diameter stainless steel cables fixed on both ends to aluminum pulleys mounted on the motors' shafts. Although the cables are very durable and rated at a minimum breaking strength of 70 lb, stretching can still occur from repetitive use. Figure 3.4 shows the motor housing and tensioning system designed to compensate for this effect: the motors are each mounted on a sliding piece of Plexiglas that can be adjusted to increase tension in the cables. One can see that other similar motors could be added into this housing to accommodate additional fingers or DOF.

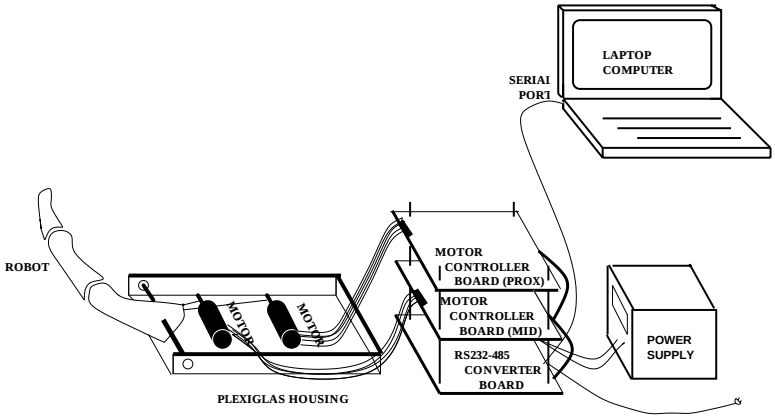

Figure 3.3: Diagram of the actuation hardware for the robot finger.

The micromotor/tendon apparatus that actuates the robot finger is shown in Figure 3.5. Note that the two motors had to be horizontally offset from each other so cables running from them would not interfere with each other.

The shaft of the motor driving the MCP joint is fitted with a 4.94 mm (0.195 in) diameter pulley. A Nylon-coated steel cable extends from this pulley to a 6.86 mm (0.270 in) diameter pulley that is pressed onto the rotational axis dowel of the MCP joint and embedded into the side of the finger. After wrapping around this pulley, the cable returns back to the motor shaft pulley. Because the proximal link and the MCP joint pulley are attached (as described in Subsection 2.2.1), the bidirectional cable acts to move the link in flexion and extension depending on the direction of the motor.

For the PIP joint, a cable extends from a 4.94 mm (0.195 in) diameter pulley fixed on the other motor shaft past an idle pulley on the MCP joint axis and up through the hollow of the proximal link. It then wraps around a 6.25 mm (0.250 in) diameter pulley and returns back down the same route, terminating at the motor shaft pulley. The idle pulley is mounted on a miniature ball bearing in order to reduce frictional effects. It serves to guide the cables, ensuring that they maintain a constant lever arm with respect to their designated axis no matter the finger posture.

Because the PIP joint tendons pass over an idle pulley in the MCP joint, the resultant torque at the MCP joint is not exclusively determined by its respective motor. This cross-axis coupling induced by

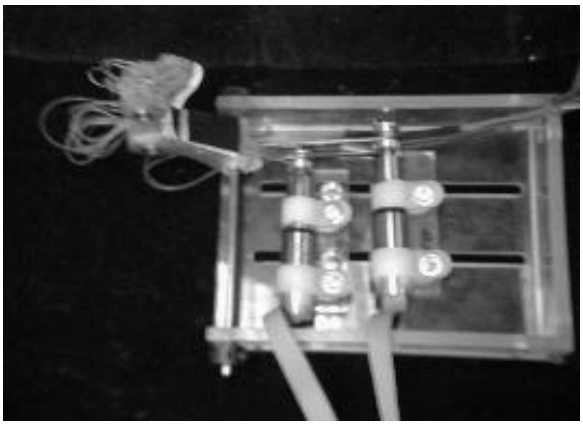

Figure 3.4: The Plexiglas motor housing and tensioning system for the robot.

cable tensions introduces motion control issues. The reader is referred to [88] for further discussion.

As shown in Figure 3.5, the DIP joint is coupled to the PIP joint by a cable anchored at both ends in the distal phalanx and routed to a pulley fixed to the axis in the head of the proximal phalanx. This arrangement effectively reduces the number of motors needed to actuate the three joints of the finger. Again, the bidirectional cabling allows for both extension and flexion.

By coupling these joints we mechanically introduce a grasping behavior: when the PIP and thus the DIP joint is flexed, the distal and middle links curl inwards, wrapping around a present object. Such behavior, though not implemented through a direct coupling, is a feature of human fingers.

3.2.1 Actuator Specifications

The MicroMo Series 1219 12 V DC motors have a 12 mm (0.472 in) diameter and are 49 mm (1.933 in) long, including the encoder and the gearhead. Selection of the motors and gearheads was based on their torque, speed, power consumption, and mechanical specifications (shown in Table 3.1 and Table 3.2). MicroMo Series HE magnetic encoders are located coaxially with each of the driving motors. They are 2-channel encoders with a resolution of 10 counts per revolution (CPR).

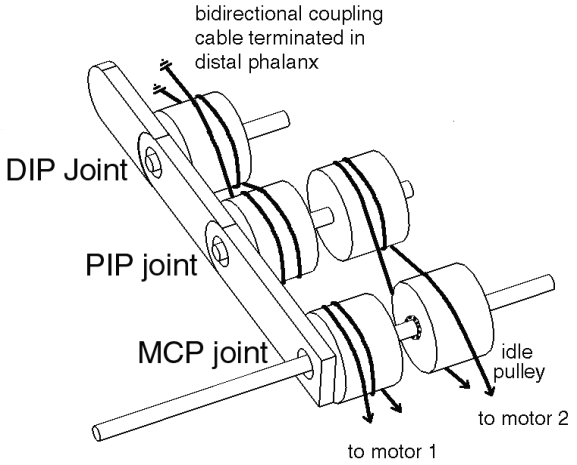

Figure 3.5: Motor/tendon/pulley transmission system.

Max. intermittent power output(Watts)	.50
Max. continuous power output(Watts)	.45
Max. efficiency	72%
No load speed(RPM)	16,000
Stall torque(oz-in)	.169
Max. continuous torque(oz-in)	.09
Weight(oz)	.39

Table 3.1: Specifications for MicroMo Series 1219 DC coreless motor.

At no load, the motors with the gearheads have a maximum angular velocity of 62.5 rpm. This corresponds to joint flexion or extension through a 90° angle in 0.24 seconds. (On average, the muscles in the human hand require 80 to 200 ms to complete a similar contraction at maximum speed.)

The motor stall torque is 0.169 oz-in. With the gearhead, this enables the robot's MCP joint to support a load of up to 0.768 lb (3.4 N) at the fingertip (a maximum moment arm of 3.7 inches (9.41 cm) from the effective joint). This is opposed to the 20–40 N and 5–10 N of force that a human finger is capable of generating in flexion and extension, respectively. However, the average person is only able to exert about 7 N with her fingertip without experiencing discomfort or fatigue [35].

Reduction ratio	256:1
Max. continuous output torque(oz-in)	14.2
Max. intermittent output torque(oz-in)	28.3
Efficiency	60%
Weight(oz)	.35
Length(in)	.748

Table 3.2: Specifications for MicroMo Gearhead Series 10/1 with 256:1 gear ratio.

The efficiency of the motor and gearhead is 43%. On the other hand, the isothermal mechanochemical processes that allow living organisms to intake energy from food and output mechanical energy for work are very different from the principles that underlie the function of engineered actuators. Such organic energy conversion can be greater than 50% efficient [25]. Muscle also has the ability to modify and repair itself in response to imposed stresses and strains. Overloading the motor will cause permanent damage.

The maximum power per unit mass (W/kg) of an actuator is also an important consideration in robotics. This figure will determine the speeds and forces that can be generated through a system's transmission apparatus. The motors used in the robot have a power density of ∼40 W/kg. Human muscle is typically about 50 W/kg, though certain muscles can reach as high as 200 W/kg for brief periods of time [57]. The close proximity of the different actuators' power densities can be misleading because, in general, electric motors operate efficiently at high speeds/low torque, while muscles operate at low speeds/high force.

Each motor is connected to a PIC-SERVO integrated motion controller/motor control board from J.R. Kerr Automation Engineering [108] that is designed to provide full-function servo control to DC motors with TTL compatible incremental 2-channel encoders. Each compact 5.3 x 7.9 mm^2 (2.1 x 3.1 in^2) board features:

- A PIC-SERVO/PIC-ENC servo motion control chipset based on PIC16Cxx series microcontrollers. The PIC-SERVO executes a PID servo control filter with optional current/output/error limiting, trapezoidal and velocity profiling, serial command interfacing, and 20KHz PWM, direction, and enable signaling. The PIC-ENC performs time critical 16-bit encoder counting.

- An LMD18201 H-bridge amplifier that can source up to 3 amps continuously, 6 amps peak at up to 48 V(DC).

- An optical encoder interface.
- A serial communications interface.
- 2 I/O bits for limit switch inputs or control outputs.
- An auxiliary analog input channel with pre-amplifier.

Through an RS485 multi-drop interface, these boards are daisy-chained together along with a RS232-485 Serial Port Converter and connected to the serial port of a laptop PC running Windows 2000. All of these modules share the same 7.5 V logic power supply. This modular configuration greatly simplifies wiring and reduces noise and overall space requirements. It allows up to 32 control modules to be commanded from a single standard serial port at baud rates from 19,200 to 115,200 bps. The communication protocol is a master/slave protocol whereby command packets are transmitted over a single dedicated line to each controller module by the host computer and the returned status packets are received over a separate line which is shared by all of the modules on the network.

The C++ motor control software uses a vendor-provided driver to interface with the motor boards through the laptops's RS-2332 port [40]. A Microsoft Foundation Classes (MFC) application implements a velocity control law based on Bounded Linear Attractors [18]:

$$V = C \times \exp^{(d/\alpha)^2/2} \times md \tag{3.1}$$

where V is the resultant velocity vector, m is the range of the potential field, and d is the position error. This type of velocity control allows for tight coupling with the tactile feedback for smoother performance (see *Chapter 5*).

Chapter 4

Tactile Sensation

The versatility of human hand functionality comes from the integration of superficial exteroception and deep proprioception, or kinesthesis, of arm and hand configurations. The former relies on different skin receptors to deliver contact pressure distribution, temperature, and force information; the latter relies on sensory organs in joints, muscles, and tendons to relay force, movement, and position data about the body's own postural state. The fusion of these two classes of information is referred to as "haptic perception." When under control of the sensory-motor system, these abilities lead to responsive and versatile active touch operations.

This research focuses on half of this haptic sensing suite, the primary goal being to implement some fundamental software and hardware tools for tactile perception of a robotic system. Because the human hand is the principal organ for reception of and reaction to this kind of information, we apply the problem to the finger of an anthropomorphic manipulator. Specifically, we investigate a technique for detecting the degree and distribution of a pressure applied to a surface skin of the robot. (This is opposed to detecting the total resultant force applied to a robot finger which is usually done with strain gauges or force-torque vector sensors, and in our opinion, is more akin to kinesthetic data.) This type of contact information can be used to extract information regarding the locus, intensity, and relative temoral pattern of contacting stimuli, enabling a robot to perceive and respond to uncertainties in the world.

As Section 4.1 points out, human taction involves perception of many different properties related to the contact conditions between the skin and the environment (e.g., thermal, microvibrational, surface

features). Therefore, over the last three decades, a variety of tactile sensor prototypes have been researched to provide a system with data analogous to one or all of those human modalities. This chapter covers only sensors and topics that, like the sensor on the robot finger, are primarily geared to variable pressure detection. We limit our definition of tactile sensors to arrays of force-sensitive surfaces that can transmit graded signals in parallel. This excludes single point and binary sensors.

4.1 Anatomic Taction: Human Skin and Exteroceptors

Perception occurs when external stimuli interact with the receptors of our senses. Touch is the most complex of the five human sense modalities, involving arrays of different nerve types and sensing elements to relay a whole body experience (as opposed to the other senses which are localized in the eyes, nose, mouth, and ears.) This distributed apparatus allows us to determine things about objects we contact such as their: bulk properties (e.g., hardness and viscoelasticity), mass distributions, textures, fine-form features, temperatures, and shapes. We can also extract data regarding the changing state of our interactions with them, like the force of a hug, incipient slip estimation, and even gravitational and inertial effects.

For this research, we are primarily interested in the subsystem of the somatosensory system that is associated with the skin and its innervating low-level nerve fibers. This subsystem deals with cutaneous spatiotemporal perception of external stimuli mostly through: mechanoreceptors (for pressure/vibration), thermoreceptors (for temperature), and nocioceptors (for pain/damage). These receptors, or tactile units, are all located in the various layers of the skin, which provides support and protection from the external environment. (We are most interested in the first of the three which refer to those low-threshold afferent sensory nerve terminals that are primarily responsive to light skin deformations.)

The skin of the hand, in particular, is highly specialized to provide detailed tactile feedback. Many studies have shown the fundamental dependence of finger dexterity on this sensory input [60, 46, 33]. The hairless (glabrous) skin on the front of the hand contains the most nerve endings which peak in density on the central whorl of the fingertips. The 17,000 mechanoreceptors in this skin, comprising Meissner corpuscles, Merkel disks, Ruffini organs, and Pacinian corpuscles, are

differentiated into classes depending on their receptive fields[1] and the speed and intensity with which they adapt to static stimuli (see Figure 4.1). These are: **Type I** with small receptive fields; **Type II** with large fields; rapid adaptors **(RA)** which have no static response; and slow adaptors **(SA)** which do not stop firing in response to a constant stimulus. The receptors also differ in terms of their numbers, densities within the subregions of the skin, and perceptive effects. Tables 4.1 and 4.2 indicate some of these properties. Though many receptive fields overlap and no two points of the skin are supplied by the same pattern of nerve fibers, the tactile sensor in this work responds most like isolated Merkel disks and Ruffini organs which have been associated with SA I and SA II, respectively.

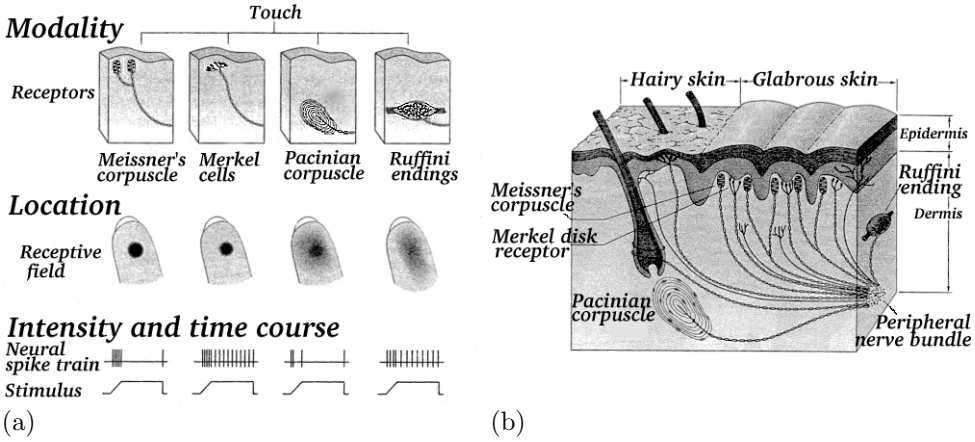

Figure 4.1: (a) The modality, location, intensity, and timing of the mechanoreceptors in the human hand. At the bottom of the diagram, a receptor's spike train indicates the action potentials evoked throughout a duration of sustained stimulation. Note that the Merkel cells and the Ruffini endings adapt slowly to the stimulus. (b) Morphology and placement of the mechanoreceptors in the skin of the human hand. Sketches adapted from [63] without permission.

As Figure 4.1*a* shows, the Merkel disks, located superficially, and the Ruffini endings in the subcutaneous tissue, are considered tonic receptors which issue a continuous rate of firing for as long as a stim-

[1]The receptive field of a receptor is defined as the area serviced by a single neuron of that receptor type. The size of this field is not absolutely fixed. It depends on the density of various sensory neurons and on the intensity and kind of mechanical stimulus present.

Table 4.1: Mechanoreceptor Characteristics

Receptor	Class	Receptive Field(mm^2)	Frequency Range(Hz)	Sensory Correlation	Receptors/ cm^2
Pacinian Corpuscle	PC	10-1000	40-800	Vibration	21
Meissner's Corpuscle	RA	1-100	10-200	Motion/Vibr.	140
Ruffini Ending	SA II	10-500	7	Skin stretch	49
Merkel Disk	SA I	2-100	0.4-100	Texture/Press.	70

Table 4.1: Quantitative characteristics of the human tactile receptors. Note data in the Sensory Correlation and Receptor fields for the biological units are considered probable, not definite. Entries for human receptors adapted from [27].

Table 4.2: Human Fingertip Specifications

Frequency Response	0-400 Hz
Response Range	0-100 g/mm^2
Sensitivity	$\approx$0.2 g/mm^2
Spatial Resolution	1.8 mm
Signal Propagation	Motor Neurons 100 m/s
	Sensory Neurons 2-80 m/s
	Automatic Neurons 0.5-15 m/s

Table 4.2: Sensory specifications of the human fingertip assembled from [32, 47, 54, 63, 68].

ulus is maintained. The former transmit compressing strain from the skin and are distributed preferentially on the distal half of the fingertip; the latter are distributed more uniformly and sense stretch of the skin around joints and fingernails, contributing to the perception of an object's shape. Although the firing of all types of receptors in parallel produces the sensation of contact with an object, the activation of these two types of receptors produces sensation of a steady pressure on the skin.

Another tactile feature of the skin is referred to as the two-point threshold. This is the minimum distance between which two simultaneous indentions can be uniquely resolved. For the index finger, this distance is 2 mm—any two stimuli closer than this will feel like a single point. (If the two stimuli are received sequentially, this interpoint threshold is finer). Such multi-point resolution is a significant issue in

regard to artificial taction. Most sensors cannot differentiate multiple stimuli at all, let alone discriminate between very close inputs. Instead they either extrapolate a virtual point, choose one, or relay erroneous information altogether.

The skin of the hand also has important mechanical properties. Estimates of the static coefficient of friction of the human fingertip skin range form 0.5-1.0 [36]. Sweat produced by glands in the skin creases provides an adhesive quality, increasing these numbers. This perspiration, as well as the viscoelastic fatty substrate lying beneath the skin, also enables the hand to be far more effective at holding rough surfaces and preventing slippage of tools than the frictional coefficients indicate.

It is clear that these multi-faceted skin properties would enhance the performance of robotic end-effectors. Thus, emerged the study of artificial tactile sensing, attempting to model the skin as an information processing field to extract static and dynamic features of touching surfaces.

4.2 Introduction to Artificial Tactile Sensing

The continuous measurement of variable contact forces that occurs during a robotic manipulator's interaction with the environment has become increasingly important in medical, industrial, design, and research applications. This is accomplished with different types of miniaturized sensors, most often embedded uniformly as matrices into elastic material on the fingertips of an end-effector. Like their various human counterparts, the individual tactile elements, or *taxels*[2], relay information about the contact status of the surface on which they are mounted.

Establishing finger-like criteria from analysis of human sensing in grasping, manual exploration, and manipulation seemed like a reasonable first approach to artificial taction. This was evidenced by Harmon's [53] follow up on an initial survey of developers and users in the field. His analysis codified a set of tactile sensor design parameters, leading up to the following list of performance specifications which is still widely referenced by researchers today. Note these are general characteristics, and like all design factors, are application dependent, not definitive. They are analogous to the biological characteristics in Table 4.2.

[2]These are also referred to as *tactels* (derived directly from 'tactile elements'). The term *taxel* is not to be confused with the texture analysis term *texel*.

- The sensor should comprise an array of sensing elements embedded in a thin, flexible substrate. The substrate and any covering should be skin-like, compliant, durable, and wear-resistant.

- The spatial resolution should be at least on the order of 1-2 mm (1/10 inch), translating to an approximately 10x15 element grid on a fingertip-sized area.

- The sensor should demonstrate high sensitivity and broad dynamic range. A single taxel's threshold sensitivity should be on the order of 1 gram and have an upper limit of 1000 grams (.01-10 N) with allowance for accidental mechanical overload. In other words, a dynamic range of 1000:1 is satisfactory.

- The sensor should provide stable, repeatable, and continuous-variable output signals. This response need not be linear (i.e., logarithmic is satisfactory), but should be monotonic and non-hysteretic. (Human skin, however, *does* exhibit a fair amount of hysteresis.)

- The frequency response of the touch-transducer should be small compared to the time of an overall control-loop cycle. The minimum bandwidth of the whole sensor should be at least 100 Hz, preferably 1 kHz. Each element should have a response time of around 1 ms, or a similar value related to the total number of elements, so that when multiplexed, the sensor can determine contact status in real-time.

- The sensor should be responsible for most of the pre-processing so as to minimize the number of output signal paths going to the CPU.

- The sensor should require low power and be relatively cheap.

Though several techniques have been adapted to fill these requirements, very little commercial success has been obtained so far. The complexity of many of the current technologies makes them hard to manufacture en masse and thus very costly. The following list provides general descriptions of the most common sensor configurations. The sensors exploit different transduction effects and materials capable of converting mechanical compression into other measurable domains.

- Resistive devices are probably the most prevalent type of tactile sensor, featuring two basic configurations. The first exploits the force-resistance characteristics of conductive elastomers and

foams. When subjected to external force, these materials exhibit predictable loss of electrical resistivity resulting from altered particle density. For the sensors, they are sandwiched between layers of polyester film on which conductive grids are printed. The intersection points of the rows and columns of the grids form sensing sites due to the intervening resistive layer.

Similarly, a force sensing resistor (FSR) is a piezoresistive polymeric material that exhibits decreased resistance when pressure is applied normal to its surface. A film consisting of electrically conducting and non-conducting particles suspended in a matrix is etched onto facing surfaces of pliable polymer sheets. The electrical resistance between the conductors is measured through the FSR polymer. FSR's have been applied to the Matsuoka [76] and DLR [23] hands from *Chapter 1.*

- Piezoelectric materials convert mechanical stress into proportionate output voltage potentials. In tactile sensors, these are usually used in the form of a polymer, such as polyvinylidene fluoride (PVF_2), which must be made piezoelectric by first exposing it to a high electric field. Such films are pyroelectric as well, responding to heat fluxes by generating electric charge. Allen et al. [5] has applied this type of sensor to the Utah/MIT Hand described in *Chapter 1.*

- Capacitative sensors rely on the fact that the capacitance of a parallel plate capacitor is a function of the areas of the two plates and the thickness of an intervening dielectric medium, i.e., the distance between the plates. Such a device responds to applied forces that change either this distance or the effective surface area of the capacitor. This type of sensor has been applied to the Utah/MIT Hand [62] as well.

- Magnetic transduction sensors often rely on mechanical movements to produce flux density changes in magnetic fields. These measurements are usually made by Hall effect sensors. Other such transducers employ magnetoresistive or magnetoelastic materials. When subjected to mechanical stress, these materials exhibit changes in their magnetic fields.

- Photoelectric, or optical, tactile sensors also come in different forms. Intrinsic devices involve modulation of some feature (e.g., optical phase, polarization, etc.) of transmitted light without

interrupting the optical path; extrinsic devices involve the interaction of stimuli external to the primary light path. The sensor used in this research is of the latter type and is fully detailed in the following sections.

We refer the reader to [65, 38, 26, 80, 49] for descriptions of other hybrid and less common sensors (based on, e.g., electrorheological fluids, carbon fibers, MEMS, etc.) as well as more detailed implementations of the aforementioned technologies.

4.3 The Robot Analogue: Tactile Sensing Components

This work was primarily motivated by the desire to investigate tactile sensing as a tool for robot manipulation. In the pursuit of this, we were made increasingly aware of the technical difficulties involved in this kind of perception—as evidenced by the lack of off-the-shelf sensors that could be used to this end.

Besides adhering to the sensitivity, dynamic response, and other specifications delineated above, the sensor needed to be able to detect simultaneous multi-point stimuli, and provide real-time active sensing for integration with motor control. It also needed to allow for easy fabrication and mounting at variable spatial resolution, and be affordable, flexible, and scalable to different sizes and irregular shapes.

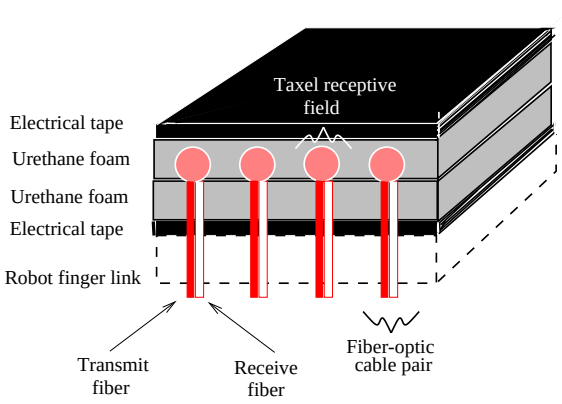

Figure 4.2: Cross-section of the tactile sensor.

.

We opted for an OEM core of a commercial multi-touch controller, the MTC-Express, manufactured by Tactex Controls, Inc. (see Table A for product specifications). The underlying contact sensing technology of the touch pad is called KINOTEX™ [89], which is a registered trademark of Canpolar East and produced under license from the Canadian Space Agency.

The technology is based on the principle of photoelasticity, whereby stress or strain causes birefringence in an optically transparent medium. Thus, the intensity of any light passed through the material changes as a function of applied force. An array of detectors, each measuring these varying intensities, effectively serves as a tactile sensor.

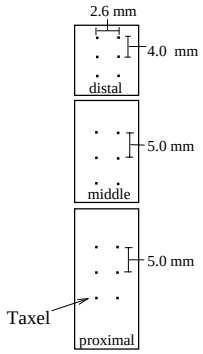

Figure 4.3: Sensor taxel arrangement on the palmar surface of the robot finger. The taxels are closer on the distal phalanx corresponding to the higher tactile resolution of the human fingertip.

Figure 4.2 shows a sketch of the implementation we use to achieve this effect. Light from an LED is introduced into an open-cell urethane foam via embedded fiber-optic cables. Because the foam is an isotropic scattering medium, a halo of illumination is projected into it from each of these *transmit* fibers. The dimensions and local intensity of this light field are determined by the absorbtion and scattering properties of the foam as well as aberrations in the fiber terminations (as described in Section 4.3.1). Another fiber-optic cable, a *receive* fiber, is placed adjacent to the transmit fiber to detect the scattered light. The other end of the receive fiber is connected to a photo-diode with associated circuitry that outputs an analog voltage corresponding to the detected load-dependent intensity. The embedded end of a transmit/receive fiber-optic cable pair constitutes a single taxel, many of which are distributed over the palmar surface of the robot in the

configuration shown in Figure 4.3. The tactile sensor thus serves as an artificial skin. (Like their biological counterparts, the tactile units refer to afferent/efferent relays whose sensory endings are primarily responsive to skin deformation and are located superficially.) An entry for a taxel can be added to Table 4.1 for comparison:

Table 4.3 (Table 4.1 revisited): Mechanoreceptor and Sensor Characteristics

Receptor	Class	Receptive Field(mm^2)	Frequency Range(Hz)	Sensory Correlation	Receptors/ cm^2
Pacinian Corpuscle	PC	10-1000	40-800	Vibration	21
Meissner's Corpuscle	RA	1-100	10-200	Motion/Vibr.	140
Ruffini Ending	SA II	10-500	7	Skin stretch	49
Merkel Disk	SA I	2-100	0.4-100	Texture/Press.	70
Sensor Taxel	~SA II	$<1.5^a$	$\approx 400^b$	Pressure	12-16

Table 4.3: Quantitative characteristics of the sensor compared to human tactile receptors.

[a] We define the receptive field of a taxel in the sensor as the circular area around which light extending from the taxel's transmitter into the surrounding foam can be sensed by its paired receiver. This is an approximate value which can vary among taxels due to the fiber-optic cable terminations, orientations with respect to the LED, local anomalies in the foam, etc. Like the receptive fields of the biological mechanoreceptors, this value is also highly dependent on the spatial density of the taxels in the whole sensor. If the density is too high, illumination of the foam becomes more uniform. In this case, light transmitted into the foam does not emanate from a point source at the taxel location and the resulting signal becomes ambiguous.

[b] This value is determined by the sampling bandwidth of the entire system, which includes the data acquisition, processing, etc. It also depends on characteristics of the foam substrate, such as the density, stiffness, and compressibility.

The artificial skin can be formed into arbitrary shapes for application to various surface geometries and sizes. It is fabricated in layers, with the top and bottom foam surfaces covered with a flexible opaque layer (currently, electrical tape) to keep out ambient light. This is needed on the bottom because the stereolithographed skeleton of the finger is translucent. The product specifications of the foam are given in Appendix A. The layered sensor construction protects the sensing elements from external hazards and provides a soft frictional surface essential for grasp stability. Note that the sensor does not span the joints of the finger. Doing so would generate erroneous pressure signals originating from the robot, not impinging contact stimuli, as the foam stretched and slackened due the robot's motion.

The hardware for the tactile sensor is depicted in Figure 4.4.

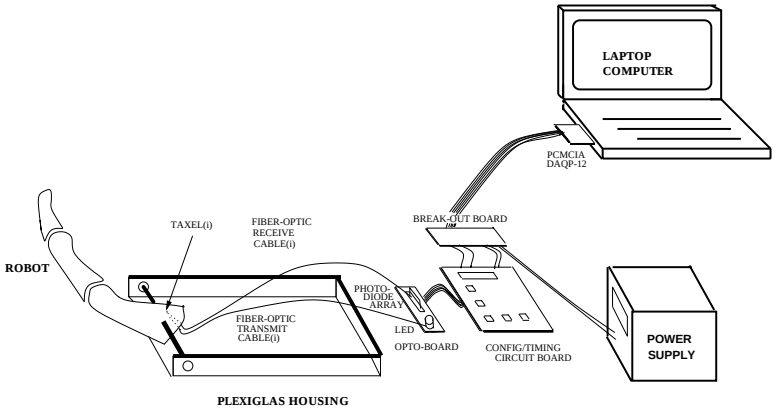

Figure 4.4: Diagram of the tactile sensor hardware for the robot. Only 1 out of 18 taxel pairs is shown.

The hardware and software for signal processing are designed such that the contact data is sent to the motion controller in real time. The OEM electronics generate all the necessary timing signals to control and sequence the sensor data as well as drive the data acquisition board (DAQP-12 from Quatech). The DAQP-12 supports up to 100kS/sec sampling at 12-bit resolution and provides 16 single-ended analog input channels, data and scan list FIFOs, trigger control, a pacer clock, and programmable channel and gain selection. The board carries out A/D conversion of the sensor signals and transmits the results to an 800 MHz laptop PC through a PCMCIA port. The PC is used for program development and to visualize, store, and perform calculations on the data for integration with the motor control software (described in *Chapter 3*).

4.3.1 Basic Lesson on Fiber-optic Cables

As described above, the tactile sensor is based on the transduction of visible light into a contact pressure signal. In our apparatus, the light is transferred from a source LED to the surface of the robot via fiber-optic cables. Such cables are currently used in many other applications in which data must be transmitted over long distances with high transmission quality and immunity from electro-magnetic and radio frequency interference. The utility of these flexible conduits is based on the phenomenon of total internal reflection (TIR).

An optical fiber is a dielectric wave guide composed of two distinct types of optically conducting material: an inner core which carries the light, surrounded by a thin cladding. The cladding has a much lower index of refraction (ratio of the speed of light in a vacuum to the speed of light in the material) than that of the core. If these indices are uniform for all cross-sections of a cable, it is referred to as a step index (SI) fiber. The fusion of the core and cladding materials creates a totally reflecting interface at their junction. The acceptance cone angle of a fiber depends on the ratio of the two indices of refraction. Light entering one end of the optical fiber within this angle zigzags down the length of the core through successive reflections off of the core/cladding interface (Figure 4.5). In contrast, much of the light entering a fiber at an angle greater than the acceptance angle will not be internally reflected, but be lost through the cladding.

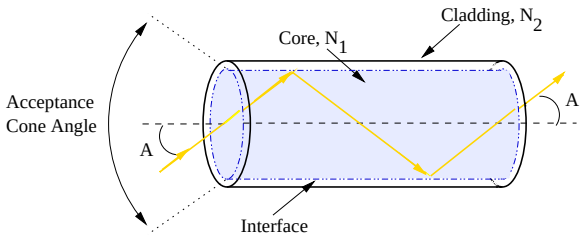

Figure 4.5: A ray of light entering at $\angle A$ within $\angle AcceptanceCone$ passes down an SI fiber-optic cable by reflecting off of the core/cladding interface. Indices of refraction for the core and cladding are N_1 and N_2, respectively, with $N_1 > N_2$.

What follows is a description of the fiber-optic cables in the current robot sensor application and some of the special considerations demanded by their use (see Appendix A for product specifications).

The fiber-optic cables used in this research are 0.250 mm diameter SI plastic optical fibers. As opposed to more common silica glass fibers that have better light transmission characteristics, plastic fibers are less expensive, more flexible, and easier to fabricate into special assemblies. These were especially important features for the current application because fiber-optic cables exhibit increasing transmission loss as a result of decreasing bend radius.

The fiber-optic cables in the robot are routed through the hollow of the finger links, weaving in and out at the joints so as not to interfere with the actuation mechanisms or get snared on moving parts. Thus, they must be able to bend along with the robot without suffering too

much variation in output intensity. The minimum bend radius is specified as 15×diameter, or a little less than 4 mm. The skeleton of the robot had to be built with this figure in mind.

Attenuation in light transmission for fiber-optic cables can be a result of other phenomena as well. Absorption and scattering can reduce the transmission 4-5% for 30.5 cm (1 foot) of cable. Our application only necessitated the fibers be on the order of 20 cm long, though this reduction would not matter because it would be consistent for the whole finger. If the sensor were to be mounted more globally, say as a skin over an entire humanoid robot, with noncontiguous areas reached by the same light source, such transmission discrepancies could be normalized out.

Light leakage due to frustrated TIR, and therefore crosstalk, can also occur between closely spaced or touching fibers. We took great care to shield adjacent fibers from each other though this would be easily resolved by using jacketed fibers which are protected by an opaque cover. This would also reduce the effects of ambient light on the fiber lengths which result in sensor readings analogous to increased pressure (because the values are measurements of intensity). Many of our experiments were done in the dark to prevent such responses. (The fiber-optic cables used in this work either came pre-attached to photodiode arrays or ferruled so we did not have the option of using jacketed cables from the start.)

In order to achieve fairly consistent "receptive fields" and no load intensities of the taxels, it was important to ensure the fiber-optic cables were not skewed, i.e., that their terminations were cut at 90° angles to their length axes. A skewed fiber effectively acts as if it has a prism on the end, causing the emitted light to diffuse irregularly, speckle, or even form a ring with a dark center. After being cut, the fiber ends were inspected under a high powered microscope to ensure the faces of the tranmit/receive fiber pairs were parallel and precise. The sensor relies on the assumption that the maximum intensity of a taxel is directly in front of the output end of the transmitter.

4.3.2 Disembodied Sensor Performance

The sensor can detect location and pressure of a contact stimulus. However, because the foam and cover distribute force-induced strains among adjacent taxels, high frequency spatial information (e.g., edges) does not translate. Furthermore, the sensor does not provide absolute deformation value, but relative changes due to the foam's viscoelastic properties.

The following plots quantify some of the sensor's performance characteristics. The data was taken with single taxels as well as small arrays of taxels in different configurations. These readings were taken on a flat surface before assembly onto the robot. *Thus the fingertip taps/presses mentioned in this discussion refer to ones actively applied to the sensor by a human subject, not to contacts generated by the robot.* The taxels in all the figures have varying initial (unloaded) values for reasons discussed above. The ramifications of these differences on sensor signal processing for motor control are discussed in *Chapter 5.*

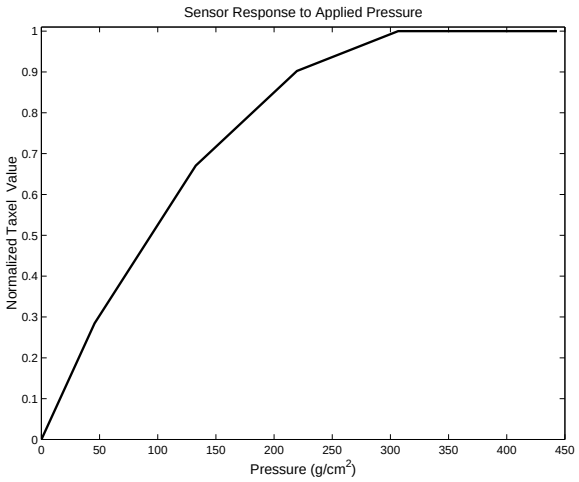

Figure 4.6: Generalized sensor response to applied pressure.

The sensor exhibits a sensitivity range of 7 g/cm^2 (calculated from response to a 3 g/42 mm^2 load) to ≈300g/cm^2. As depicted in Figure 4.6, the upper limit of this range is determined by the compressibility of the foam. At lower contact forces, displacements in the foam are easily detected. However, once the applied pressure exceeds a threshold, the foam is incapable of further displacement so the sensor readings level off.

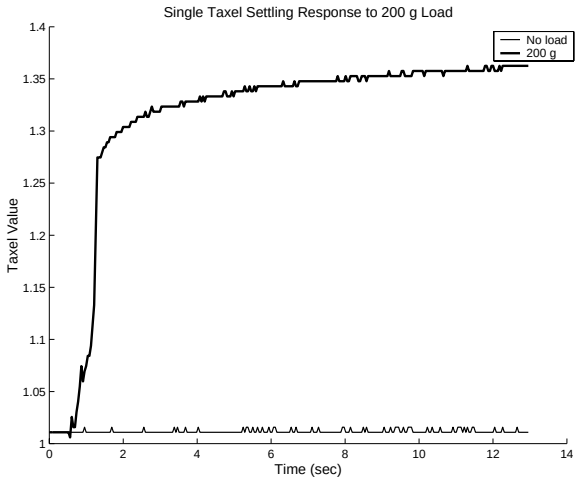

Figure 4.7: Time response of a single taxel to a 200-gram load. Signal noise can be seen on each trajectory.

The plot in Figure 4.7 shows the time it takes for a single taxel to output a stable signal in response to a 200-gram load (distributed over the area of a dime (230 mm^2)).

Figures 4.8 and 4.9 demonstrate the hysteresis inherent to the system. This is due to the viscoelastic properties of the foam. The first figure shows the state-dependent response of a single taxel in two ways: a) the response to a 200-gram load decreases with increasing total load; and b) the response to subtraction of a 200-gram load is hysteretic in that it does not return to its prior value at the same total load. This data was obtained by placing a 200-gram weight on the sensor, plotting the results, adding another 200-gram weight, plotting the results on the same graph, etc. up to a total of 800 grams. The weights were then removed one by one and the sensor responses plotted in the same fashion. In the second of the two figures, a short, large load application results in an offset from the initial unloaded signal.

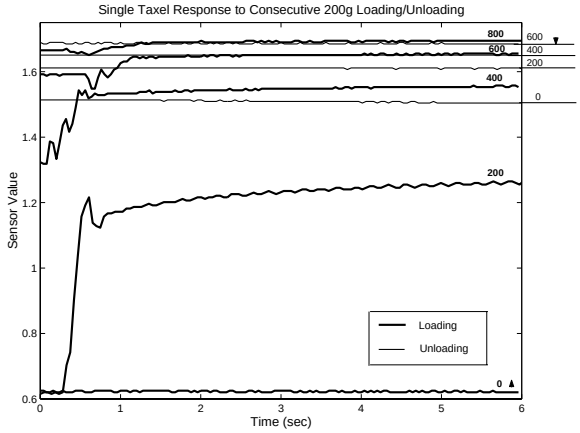

Figure 4.8: Response of a single taxel to consecutive 200-gram loads followed by their consecutive removal. Note the hysteresis.

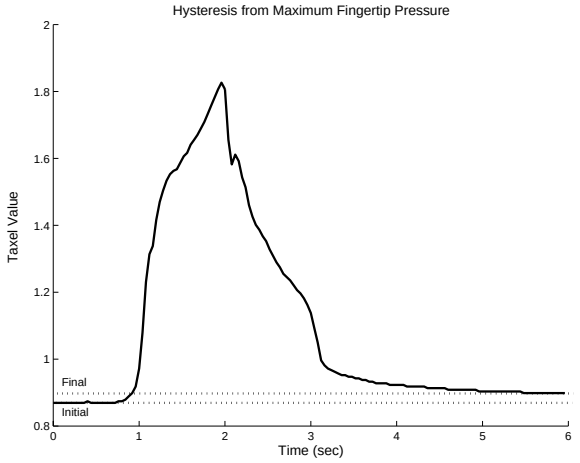

Figure 4.9: Hysteretic taxel response to maximum fingertip pressure.

As described in the previous sections, multi-point detection is an important feature of the tactile sensor. The following array tests were made on the taxel configuration exhibited in Figure 4.10. Figures 4.11*a* & *b* show taxel array responses to two stimuli. The stimuli in Figure 4.11*a* are coincident in time and duration, but differ in location and magnitude; the stimuli in Figure 4.11*b* differ in time, location, and magnitude. This plot is condensed onto one graph so as to give a more unified perspective of the taxel array.

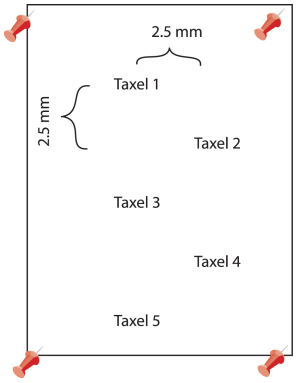

Figure 4.10: Taxel array configuration for sensor experiments.

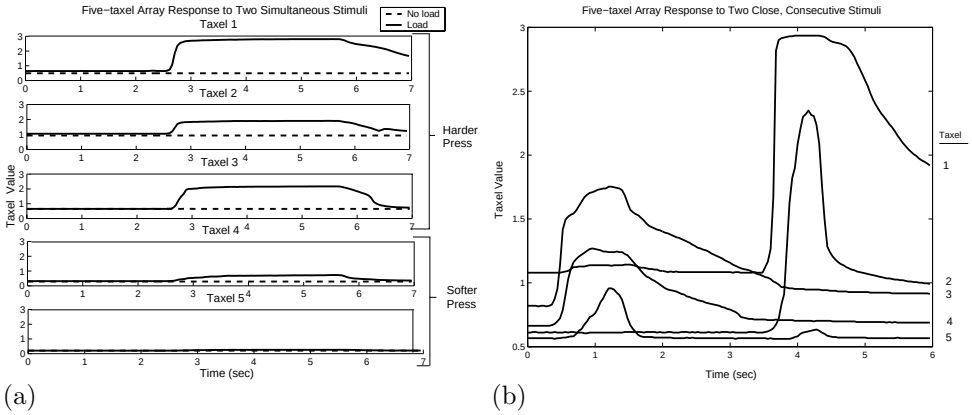

(a) (b)

Figure 4.11: Taxel array response to: (a) two simultaneous stimuli with different magnitudes and (b) two consecutive stimuli with different magnitudes (responses condensed on to one plot).

Figures 4.12 through 4.15 show taxel responses to time-varying loads.

Velocity of a stimulus can be derived from the time derivative of its contact position. The time course of a human fingertip slowly moving over an array of taxels is demonstrated in Figure 4.16.

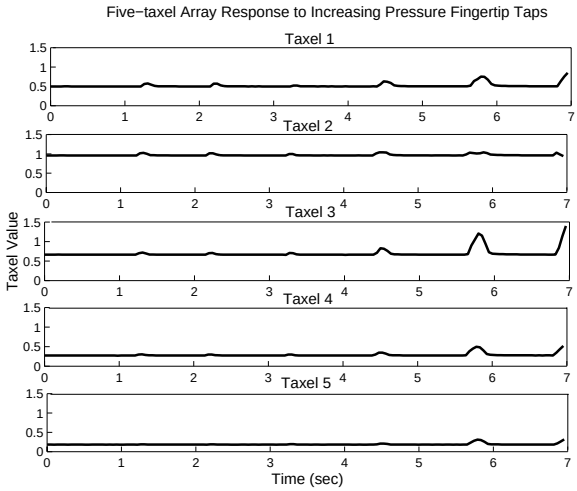

Figure 4.12: Five-taxel array response to a pattern of increasing pressure fingertip taps.

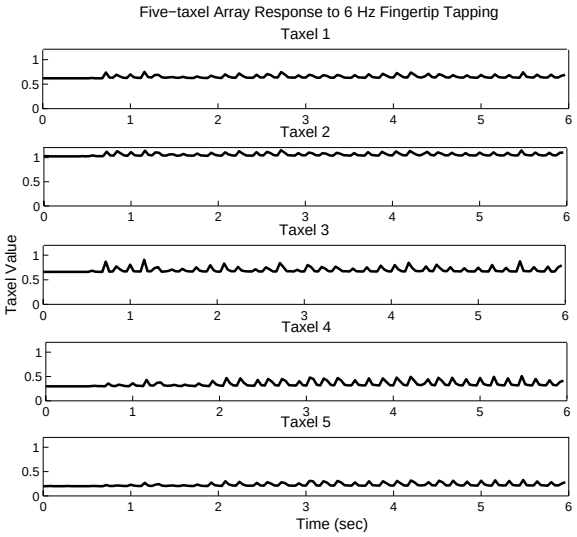

Figure 4.13: Taxel array response to fingertip tapping.

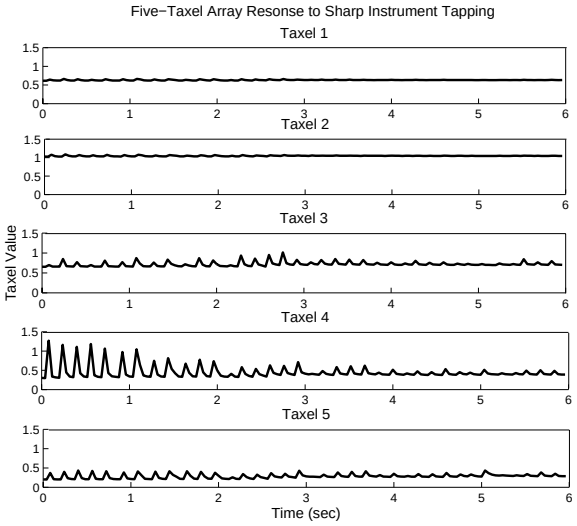

Figure 4.14: Taxel array response to sharp instrument tapping.

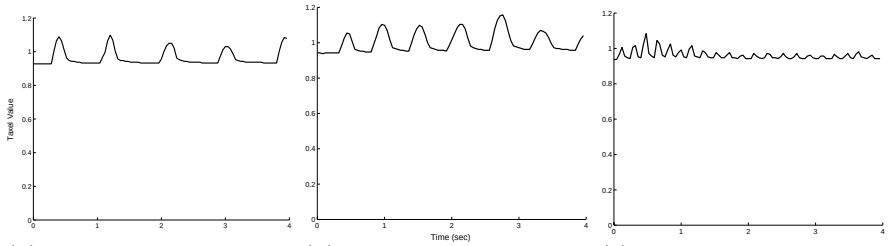

(a) (b) (c)

Figure 4.15: Single taxel response to (a) slow, (b) moderate, and (c) fast fingertip tapping.

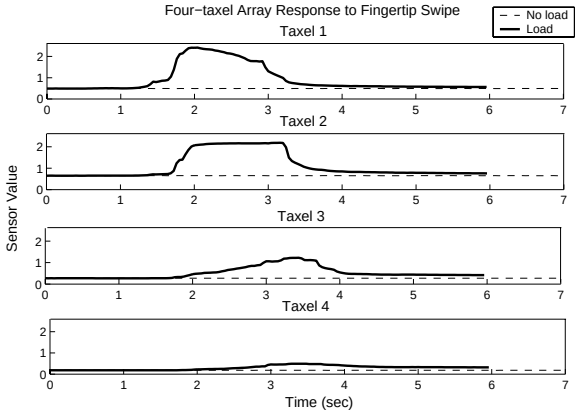

Figure 4.16: Path of a moving, decreasing pressure across an array of taxels. The taxel configuration is the same as that used in the above tests except for the exclusion of Taxel 5.

Chapter 5

An Action-Perception Example

This chapter outlines a very basic sensorimotor control scheme and experimental evidence of the general utility of tactile feedback. Because this research is mainly focused on the sensor and its potential applications, the control is initially very simple. However, the system is set up to accommodate a wide variety of behaviors reliant on surface contact information.

5.1 Introduction to Dexterous Manipulation

Dexterity is a rather broad concept in common language, that involves aspects of ability and stability in performing motions of the manipulated object by means of the hand [12]. In its application to robotics research, the term takes on a more definitive meaning that umbrellas a hierarchy of specific behaviors. Ideally, a dexterous end-effector should be able manipulate, or change the position and orientation of, an object from one reference configuration to another arbitrarily chosen one with specified contact points. This ability is contextually related to grasping and regrasping, fixturing (i.e., tightly securing), exploration, recognition, and precision control of an object in the hand workspace.

The ease and continuity with which the human hand can accomplish these functions is owed in great part to its sensing abilities. (Even in cases where touch sensation is slightly impaired, strength has to be increased to provide greater sensory feedback.) Neglecting such per-

ception, partially or totally, in a robot system dramatically reduces its performance. As an analogous baseline, manipulators without sensors must use more force than humans in order to handle the equivalent loads.

Touch sensing for a robot differs from other sense modalities (e.g., vision) because acquiring the perception involves direct interaction and contact with the environment. This imposes a certain level of difficulty on the a control system which must make use of active, rather than passive information. Roboticists have uncovered a wealth of issues in regard to implementing such control, from the contact and frictional properties of hard versus soft fingers, to analysis of rolling, sliding, and slipping feedback.

We are primarily interested in grasping, which can essentially be considered a low-level task compared to high-level manipulation and recognition tasks which involve both perception of and conscious reasoning about object features. Of course there are many elements (e.g., attentiveness, intent, novelty) that dictate the initiation of a grasp. We however, further limit the scope to reflexive grasping elicited in reaction to a tactile stimulus. Such habitual maneuvers make no corrections for stability and do not vary over the breadth of possible configurations or force outputs. They are akin to the manual reflexes of infants (except that the robot doesn't use a palm surface like children do.)

5.2 Human Dexterity: the Systematic Emergence of Coordination

This section is not meant to provide a picture of the action-perception system responsible for human dexterity, especially because we make no attempt to model this apparatus. Instead, we couch our work in a developmental process that begins in utero.

The manual coordination that the human sensorimotor system begets does not just spring to life. Though many of the physical and neural components involved are present and functional at birth, they are neither fully developed or connected. This is intuitively appropriate, for a highly capable baby without commensurate experience or understanding of her surroundings would be a danger to herself. Instead, infancy is a period of initially limited capacities and reflexes that allow the child to engage in safe and effective interactions with the environment. These reflexes, controlled by the spinal cord, eventually become subsumed in or replaced by more complex actions and behaviors. Piaget [84] is well-known for his assessment of this rudimentary *sensorimotor*

stage of development and of how early reflex-derived schemas become increasingly differentiated with experience.

The palmar reflex emerges when the baby is still in the womb and is inhibited around 2-4 months after birth. This reflex is activated by stimulation of the child's palm and results in flexion of the fingers. Thus, it allows the baby to practice grasping and letting go of objects. As the process repeats itself the central nervous system forms connections between the actions and perceptions that express manipulative learning. We are interested in reproducing a similar reflex on the robot, both as an example of tactile sensation dependent motion and as a tool for bootstrapping "voluntary" manipulation routines.

5.3 The Robot Analog: Sensor-based Finger Control

As described in the previous chapters, the tactile signals are integrated with the motor control software in a laptop computer. The software is implemented in the Visual Studio C++ programming environment. Figure 5.1 depicts all the hardware modules involved in the sensorimotor control of the robot. Figure 5.2 shows the robot with the tactile sensor intact in a possible grasp configuration.

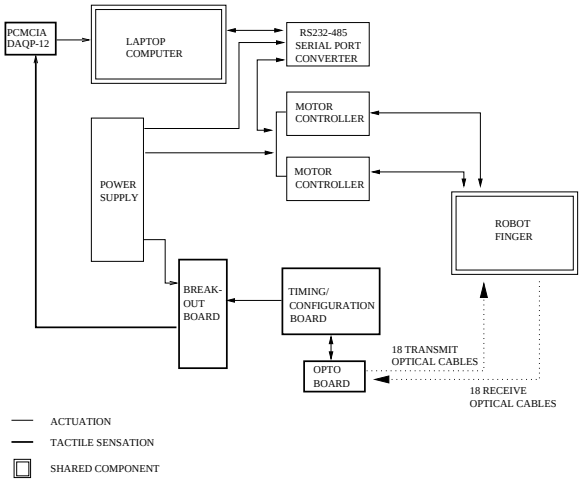

Figure 5.1: Sensorimotor control modules of the robot.

We implement position controlled actions based upon the outcome

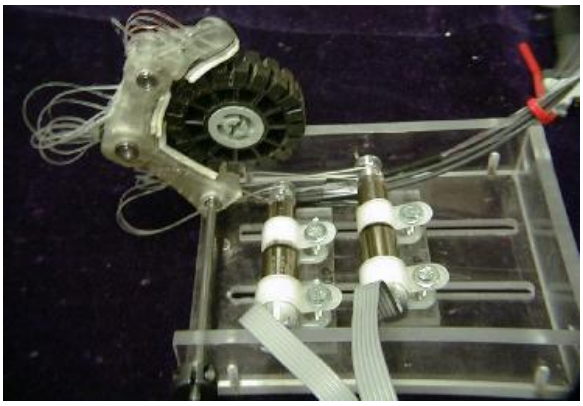

Figure 5.2: Photo of the robot grasping an object.

of tactile signal processing. A touch sensation a finger link activates with both motors to a predefined grasp position. The touch is defined by a specified array of taxels eliciting a response above an experimentally determined threshold. If this touch response remains above the threshold from one sample to the next, an object is considered to be held within the envelope of the finger. When the combined response drops below this value, the contact is considered lost and the robot extends.

Because the robot is a planar configuration made of a semi-brittle polymer, it is only presented with objects that do not exceed its torque, balance, or stress limitations. Under these circumstances the control scheme proved simple and robust.

The diagram in Figure 5.3 represents a finite state machine (FSM) for implementing a broader set of reactions to tactile stimuli. It allows for grasp and "pain" reflexes, as well as increments of increasing output force to correct for slight object perturbations. The states of the FSM refer to actions and resulting configurations of the robot and the transitions refer to perceptions of different tactile stimuli. For instance if both joint are extended, as in *Extend MCP/PIP* and the robot registers a touch (defined by a sustained, diffuse contact), both joints will flex to grasp a presented object. From here, if the object is displaced from its initial orientation by external force, the sensor will register a motion (slip) and the robot will tighten its hold by increasing flexion of its PIP joint. An especially important feature depicted in this FSM is a self-protective pain reflex, which causes the robot to withdraw from the stimulus. The percept of pain refers to a focused, high force stimu-

lus such as that incurred by a sharp instrument that could damage the sensor. This concept of self-preservation actions could be of great use to robotic system in terms of maintenance as well as more advanced learning.

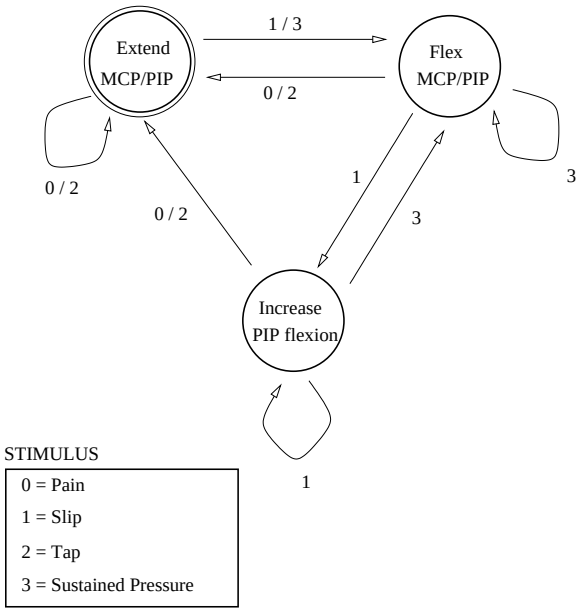

Figure 5.3: FSM of a control scheme allowing for grasping and pain reflexes, as well as increasing, incremental force outputs with object displacement.

Chapter 6

The Future

Throughout the course of this research, ideas for future design changes and far-reaching goals presented themselves. Most of the fabrication challenges for the robot were due to its small form factor. This made routing the fiber-optic cables and installing the actuating tendons painstaking endeavors. (Though the size of the robot is also a redeeming feature, as it proves viable tactile sensing and actuation can be done on a limited scale. This is an especially cogent argument for the use of this type of sensor in prosthetic devices.) Increasing the dimensions of the finger would allow for experimentation with different actuation techniques as well as the inclusion of a broader sensing suite. The finger could then more easily accommodate another degree of freedom (roll) in the MCP joint as well.

The fact that the robot was constructed directly from stereolithographed pieces meant it was too fragile to sustain heavy loads or hard impacts. Besides constraining grasp experiments, the skeleton's vulnerability necessitated extra handling care and "accident-proofing" of the lab space. Having the finger links cast in aluminum or RP'd out of a more robust, non-polymeric material would increase the robot's functionality. This would have to be done before the robot could be integrated into a whole hand capable of appropriate humanoid strength.

Incorporating intentional mechanical compliance into the finger joints would enable the use of other sensors for deriving "kinesthetic" information. This would allow for dynamic force control of the robot's motions as it interacted with the environment. The control could also be developed using learning algorithms to auto-associate the sensor feedback with particular grasp configurations. The resulting behaviors would resemble the developmental progression from reflexes to voluntary ac-

tions, such as exploration, object recognition, and manipulation.

The sensor, in particular, could be expanded to all sides of the robot. A fingernail could then be embedded in it. Like its biological counterpart, the nail would be an important information transducer with which the robot could scrape, dig, and tap objects. The detail of a tactile image is in part limited by the cover of the foam, which acts as a mechanical low-pass filter by distributing load applications. These effects may be reduced by instead using a pigmented polymer coating that can be painted on.

Furthermore, the tactile sensor need not rely on fiber-optic cables to transmit light into the scattering medium. Using diffuse backlighting in concert with just the receive fibers would half the amount of connections needed. In this case, the base response of each taxel would be a function of its distance from a single, stationary source. This type of configuration would help to smooth out no load taxel responses that are in part determined by the orientation of the receiver fiber with respect to the source LED.

Appendix A

Sensor Material and Peripheral Hardware Specifications

PORON® Foam Characteristics

Manufacturer	Rogers Corporation
Product ID#	4701-50-20-062-33
Density	320 kg/m^3
Thickness	0.20 cm
Formulation	High Modulus (firm)
Compression Force Deflection	90-159 kPa
Color	Neutral

Table A.1: PORON® product specifications from [34]. It was especially important that the foam be of neutral color, not black, as it is commonly manufactured. The dark color does not scatter the light and renders the sensor ineffective.

Lumileen® Fiber-optic Cable Specifications

Manufacturer	Poly-Optical Products, Inc.
Nominal Diameter	0.250 mm
Type	Step-index Fiber
Grade	Industrial
Core Material	Polymethyl Methacrylate
Core Refractive Index	1.495
Cladding Material	Fluorinated Polymer
Cladding Refractive Index	1.402
Acceptance Cone Angle	$60^{/circ}$
Min. Bend Value	15xDiameter
Percent Core	95-98%

Table A.2: Lumileen® product specifications from [86].

MTC-Express Touchpad Specifications

Manufacturer	Tactex Controls, Inc.
Licensor	Canadian Space Agency
Active Tablet Area(in, W×D)	5.75×3.75
Weight(oz)	17.0
Min. Activation Pressure(psi)	0.4
Max. Indentation(in)	0.08
Noise/Vibration Emissions	None
Horizontal Pointing Accuracy(in)	0.05
Operating Power Req.(VDC)	120 VAC, 60 Hz, 8 W
Sampling Rate(Hz)	200
Pressure Resolution	8 bits
Interface	RS-232 Serial, 115 KBaud
Connector	DB9
Operating Temperature(C)	35 to +100

Table A.3: MTC-Express product specifications summarized from [1].

Bibliography

[1] Mtc-express product specifications. Tactex Controls, Inc., 2000.

[2] M. Alam, C. Mavroidis, N. Langrana, and P. Bidaud. Mechanism design using rapid prototyping. In Proc. of the 10th World Congress on the Theory of Machines and Mechanisms, Oulu, Finland, 1999.

[3] H. Aldridge, W. Bluethmann, R. Ambrose, and M. Diftler. Control architecture for the robonaut space humanoid. In First IEEE-RAS Int. Conf. on Humanoid Robots, Cambridge, MA, September 2000. IEEE-Robotics and Automation Society.

[4] M.S. Ali, K.J. Kyriakpooulos, and H.E. Stephanou. The kinematics of the Anthrobot-2 dextrous hand. In IEEE Int. Conf. on Robotics and Automation Proc., volume 3, pages 705–710, 1993.

[5] P. K. Allen, P. Michelman, and K. S. Roberts. A system for programming and controlling a multisensor robotic hand. In IEEE Transactions on Systems, Man, and Cybernetics, volume 20, pages 1450–1456, November 1990.

[6] K. N. An and E. Y. Chao. Activities at the mayo clinic biomechanics laboratory. In Proc. of the 24th Rocky Mountain Bioengineering Symposium, volume 23, pages 1–7, 1987.

[7] K. N. An, E. Y. Chao, W. P. Cooney III, and Ronald L. Linscheid. Normative model of human hand for biomechanical analysis. Journal of Biomechanics, 12:775–788, 1979.

[8] S. Ashley. Rapid prototyping is coming of age. Mechanical Engineering, 63, July 1995.

[9] Henry Dreyfus Associates. The Measure of Man and Woman. Whitney Library of Design, New York, NY, 1993.

[10] J. L. Banks. Novel design and control of an anthropomorphic robotic finger. Master's Thesis Proposal.

[11] Jeff C. Becker and Nitish V. Thakor. A study of the range of motion of human fingers with application to anthropomorphic design. In Proc. of IEEE Transactions on Biomedical Engineering, volume 35, February 1988.

[12] A. Bicchi. Hands for dextrous manipulation and powerful grasping: A difficult road towards simplicity. In IEEE Trans. Robotics and Automation, volume 16, December 2000.

[13] V. Braitenberg. Vehicles: experiments in synthetic psychology. MIT Press, 1984.

[14] C. L. Breazeal. Sociable Machines: Expressive Social Exchange Between Humans and Robots. PhD thesis, Massachusetts Institute of Technology, 2000.

[15] D. Brock and S. Chiu. Environment perception of an articulated robot hand using contact sensors. In Proc. of ASME Winter Annual Meeting, pages 1–8, Miami, FL, 1985.

[16] N. Brook, J. Mizrahi, M. Shoham, and Y. Dayan. A biomechanical model of index finger dynamics. Medical Engineering Physics, 17(1):54–63, 1995.

[17] R. Brooks. Prospects for human level intelligence for humanoid robots. In Proc. of the 1st Int. Symposium on Humanoid Robots, pages 17–24, Tokyo, Japan, October 1996.

[18] R. Brooks and C. Breazeal. Embodied intelligence. MIT 6.836 text.

[19] B. Buchholz and T. J. Armstrong. A kinematic model of the human hand to evaluate its prehensile capabilities. Journal of Biomechanics, 25(2):149–162, 1992.

[20] Bryan Buchholz, Thomas J. Armstrong, and Steven A. Goldstein. Anthropometric data for describing the kinematics of the human hand. Ergonomics, 35(3):261–273, 1992.

[21] H. J. Buchner, M. J. Hines, and H. Hemami. A dynamic model for finger interphalangeal coordination. Journal of Biomechanics, 21(6):459–468, 1988.

[22] M. Buss and H. Hashimoto. Dextrous robot hand experiments. In Proc. of IEEE Int. Conf. on Robotics and Automation, page 1686, 1995.

[23] J. Butterfass, G. Hirzinger, S. Knoch, and H. Liu. DLR's multisensory articulated hand, part 1: Hard- and software architecture. In Proc. of the 1998 IEEE Int. Conf. on Robotics and Automation, pages 2081–2086, Leuven, Belgium, May 1998.

[24] A. Caffaz, G. Casalino, G. Cannata, G. Panin, and E. Massucco. The DIST-hand, an anthropomorphic, fully sensorized dextrous gripper. In First IEEE-RAS Int. Conf. on Humanoid Robots, Cambridge, MA, September 2000. IEEE-Robotics and Automation Society.

[25] D. G. Caldwell. Pseudomuscular actuator for use in dextrous manipulation. Medical and Biological Engineering and Computation, 28:595–600, 1990.

[26] D. G. Caldwell and C. Gosney. Enhanced tactile feedback (teletaction) using a mulit-functional sensory system. In Proc. of the IEEE Int. Conf. on Robotics and Automation, volume 1, pages 955–960, 1993.

[27] D. G. Caldwell, N. Tsagarakis, and A. Wardle. Mechano-thermo and proprioceptor feedback for integrated haptic feedback. In Proc. of the IEEE Conf. on Robotics and Automation, pages 2491–2496, Albuquerque, NM, April 1997.

[28] E. Y. Chao, K. N. An, W. P. Cooney III, and R. L. Linscheid. Muscle and joint forces in the hand. In Biomechanics of the Hand: a Basic Research Study [29], pages 53–72.

[29] E. Y. Chao, K. N.An, and W. P. Cooney IIIand R. L. Linscheid. Biomechanics of the Hand: a Basic Research Study. World Scientific Publishing Co. Pte. Ltd., 1989.

[30] E. Y. Chao, J. D. Opgrande, and F. E. Axmear. Three-dimensional force analysis of finger joints in selected isometric hand functions. Journal of Biomechanics, 9, 1976.

[31] J. A. Coelho, J. Piater, and R. Grupen. Developing haptic and visual perceptual categories for reaching and grasping with a humanoid robot. In First IEEE-RAS Int. Conf. on Humanoid Robots, Cambridge, MA, September 2000.

[32] P. Coiffet. Robot technology, volume 2. Prentice-Hall, 1981.

[33] D. F. Collins, B. Knight, and A. Prochazka. Contact-evoked changes in EMG activity during human grasp. Journal of Neurophysiology, 81:2215–2225, 1999.

[34] Rogers Corporation. Standard industrial materials typical physical properties. Product Pamphlet.

[35] R. M. Crowder. Local actuation of multijointed robotic fingers. In Proc. of Int. Conf. on Control, volume 1, pages 48–52. IEEE, 1991.

[36] M. R. Cutkosky, J. M. Jourdain, and P. K. Wright. Skin materials for robotic fingers. In Proc. of theIEEE Int. Conf. on Robotics and Automation, pages 1649–1654, Raleigh, NC, March 1987.

[37] M. R. Cutkosky and P. K. Wright. Modeling manufacturing grips and correlations with the design of robotic hands. In Proc. of the IEEE Int'l Conf. on Robotics and Automation, pages 1533–1539, 1986.

[38] P. Dario, A. Sabatini, B. Allotta, M. Bergamasco, and G. Buttazzo. A fingertip sensor with proximity, tactile, and force sensing capabilities. In Proc. of the IEEE Workshop on Intelligent Robots and Systems, pages 883–889, 1990.

[39] M. Ebner and R. S. Wallace. A direct-drive hand: Design, modeling and control. In Proc. of IEEE Int. Conf. on Robotics and Automation, pages 1668–1673, 1995.

[40] A. Edsinger. Dirty red: Natural movement in a mechanical spine. http://www.ai.mit.edu/people/edsinger/Papers/DR6836.htm, May 2000.

[41] A. Edsinger and Una-May OŔeilly. Personality through faces for humanoid robots. In Proceedings of ROMAN 2000 Workshop, Osaka, Japan, September 2000. IEEE.

[42] A. E. Flatt. Grasp. In BUMC Proceedings, volume 13, pages 343–248, 2000.

[43] M. Folgheraiter and G. Gini. Blackfingers: an artificial hand that copies human hand in structure, size, and function. In First IEEE-RAS Int. Conf. on Humanoid Robots, Cambridge, MA, September 2000. IEEE-Robotics and Automation Society.

[44] J. W. Garrett. Anthropometry of the hands of female air force flight personnel. Technical Report AMRL-TR-69-26, Aerospace Medical Research Laboratory, Aerospace Medical Division, Air Force Systems Command, Wright-Patterson Air Force Base, OH, 1970.

[45] J. W. Garrett. Anthropometry of the hands of male air force flight personnel. Technical Report AMRL-TR-69-42, Aerospace Medical Research Laboratory, Aerospace Medical Division, Air Force Systems Command, Wright-Patterson Air Force Base, OH, 1970.

[46] M. Gentilucci, I. Toni, E. Daprati, and M. Gangitano. Tactile input of the hand and the control of reaching to grasp movements. Experimental Brain Research, 114:130–137, 1997.

[47] G. Gordon, editor. Active Touch: the Mechanism of Recognition of Objects by Manipulation. Pergamon, Oxford, 1987.

[48] H. E. Griffiths. Treatment of the Injured Workman. Lancet, 1943.

[49] R. A. Grupen, T. C. Henderson, and I. D. McCammon. A survey of general-purpose manipulation. Int. Journal of Robotics Research, 8(1):38–61, February 1989.

[50] G. Guo, W. A. Gruver, and X. Qian. A new design for a dextrous robotic hand mechanism. In Proc. of IEEE Int. Conf. on Systems, Man, and Cybernetics, Charlottesville, VA, October 1991.

[51] F.R.S. H. Gray. Gray's Anatomy: The Illustrated Running Press Edition of the American Classic. Running Press, Philadelphia, PA, 1974.

[52] L. D. Harmon. Touch-sensing technology: A review. Technical Report MSR80-03, Society of Manufacturing Engineers, Dearborn, MI, 1980.

[53] L. D. Harmon. Automated tactile sensing. The Int. Journal of Robotics Research, 1(2):3–31, 1982.

[54] L. Heimer. The human brain and spinal cord. Springer-Verlag, 1983.

[55] G. Hirzinger et al. A mechatronics approach to the design of light-weight arms and multifingered hands. In Proc. of the 2000 IEEE Int. Conf. on Robotics and Automation, pages 46–54, San Francisco, CA, April 2000.

[56] J.M. Hollerbach, Ian W. Hunter, and J. Ballantyne. A comparative analysis of actuator technologies for robotics. Design, Technology, and Applications, 1991.

[57] I. W. Hunter and S. Lafontaine. A comparison of muscle with artificial actuators. In IEEE Solid-State Sensor and Actuator Workshop, pages 178–165, 1992.

[58] Canpolar East Inc. Kinotex configuration basics. Confidential document, February 2000.

[59] S. C. Jacobsen, J. E. Wood, D. F. Knutti, and K. B. Biggers. The UTAH/MIT dextrous hand: Work in progress. In Robot Grippers, pages 341–389, Springer-Verlag, Berlin, 1986.

[60] R. S. Johansson and G. Westling. Roles of glabrous skin receptors and sensorimotor memory in automatic control of precision grip when lifting rougher or more slippery objects. Experimental Brain Research, 56:550–564, 1984.

[61] M. Johnson. The Body in the Mind & the Bodily Basis of Meaning, Imagination, and Reason. The University of Chicago Press, Chicago, Illinois, 1987.

[62] D. Johnston, P. Zhang, J. Hollerbach, and S. Jacobsen. A full tactile sensing suite for dextrous robot hands and use in contact force control. In Proc. of IEEE Int. Conf. on Robotics and Automation, pages 3222–3227, Minneapolis, MN, April 1996.

[63] E. R. Kandel, J. H. Schwartz, and T. M. Jessell. Principles of Neural Science. The McGraw-Hill Companies, Inc., New York, 4 edition, 2000.

[64] I.A. Kapandji. The Physiology of the Joints, volume 1. E&S Livingstone, Edinburgh and London, 2 edition, 1970.

[65] G. L. Kenaley and M. R. Cutkosky. Electrorheological fluid-based robotic fingers with tactile sensing. In Proc. of the IEEE Int. Conf. on Robotics and Automation, volume 1, pages 132–136, Scottsdale, AZ, 1989.

[66] G. Lakoff. Women, Fire, and Dangerous Things: What Categories Reveal about the Mind. The University of Chicago Press, Chicago, Illinois, 1987.

[67] T. Laliberte, C. Gosselin, and G. Cote. Rapid prototyping of mechanisms. In Proc. of the 10th World Congress on the Theory of Machines and Mechanisms, Oulu, Finland, 1999.

[68] L. L. Langley, I. R. Telford, and J. B. Christensen. Dynamic Anatomy and Physiology. McGraw-Hill, 1974.

[69] C. Laschi, P. Dario, M. C. Carrozza, Eugenio Guglielmelli, et al. Grasping and manipulation in humanoid robotics. In First IEEE-RAS Int. Conf. on Humanoid Robots, Cambridge, MA, September 2000. IEEE-Robotics and Automation Society.

[70] S. J. Lederman and R. L. Klatzky. The intelligent hand: An experimental approach to human object recognition and implications for robotics and AI. AI Magazine, 15(1):26–38, 1994.

[71] F. Leoni, M. Guerrini, C. Laschi, David Taddeucci, Paolo Dario, and Antonina Starita. Implementing robotic grasping tasks using a biological approach. In Proc. of IEEE Int. Conf. on Robotics and Automation, pages 2274–2280, Leuven, Belgium, May 1998.

[72] J. W. Littler. On the adaptability of man's hand (with reference to the equiangular curve). The Hand, 5:187–191, 1973.

[73] C.S. Lovchik and M.A. Diftler. The robonaut hand: A dextrous robot hand for space. In Proc. of the 1999 IEEE Int. Conf. on Robotics and Automation, pages 907–912, Michigan, May 1999.

[74] J. N. Marcincin, L. Karnik, and J. Niznik. Design of the intelligent robotics systems from the biorobotics point of view. In Proc. of the IEEE Int. Conf. on Intelligent Engineering Systems, pages 123–128, 1997.

[75] M. T. Mason and Jr. J. K. Salisbury. Robot Hands and Mechanics of Manipulation. MIT Press, Cambridge, MA, 1985.

[76] Y. Matsuoka. Embodiment and manipulation learning process for a humanoid robot. Master's thesis, Massachusetts Institute of Technology, May 1995.

[77] E. D. McBride. Disability Evaluation. T. B. Lippincott Co., 1942.

[78] Y. Nakano, M. Fujie, and Y. Hosada. Hitachi's robot hand. Robotics Age, 6(7), July 1984.

[79] J. Napier. The prehensile movements of the human hand. Journal of Bone and Joint Surgery, 38B(4):902–913, November 1956.

[80] H. R. Nicholls. Tactile sensor designs. In H. R. Nicholls, editor, Advanced Tactile Sensing for Robotics, volume 5 of World Scientific Series in Robotics and Automated Systems, pages 13–48. World Scientific Publishing Co. Pte. Ltd, 1992.

[81] M.R. Nicholls and M.H. Lee. A survey of robot tactile sensing technology. Int. Journal of Robotics Research, 8(3):3–30, 1989.

[82] A. M. Okamura, N. Smaby, and M. R. Cutkosky. An overview of dextrous manipulation. In Proc. of ICRA 2000 Symposium on Dextrous Manipulation, 2000.

[83] M. Otake, M. Inaba, and H. Inoue. Kinematics of gel robots made of electro-active polymer PAMPS gel. In Proc. of the 2000 IEEE Int. Conf. on Robotics and Automation, pages 488–493, San Francisco, CA, April 2000. IEEE.

[84] J. Paiget. The Grasp of Consciousness: Action and Concept in the Young Child. Harvard University Press, Cambridge, MA, 1976.

[85] C. Pellerin. The salisbury hand. Industrial Robot, 18(4):25–26, 1991.

[86] Inc. Poly-optical Products. Technical Manual.

[87] A. K. Poznanski. The Hand in Radiologic Diagnosis. W. B. Saunders, Philadelphia, 1974.

[88] J. Pratt. Exploiting Inherent Robustness and Natural Dynamics in the Control of Bipedal Walking Robots. PhD thesis, Massachusetts Institute of Technology, Cambridge, MA, 2000.

[89] E. M. Reimer and L. Danisch. Us5917180: Pressure sensor based on illumination of a deformable integrating cavity. Delphion Intellectual Property Network, June 1999. Patent.

[90] D. W. Robinson, J. E. Pratt, D. J. Paluska, and G. A. Pratt. Series elastic actuator development for a biomimetic walking robot. In Proc. of Int. Conf. on Advanced Intelligent Mechatronics, pages 561–568. IEEE/ASME, September 1999.

[91] R. N. Rohling and J. M. Hollerbach. Modelling and parameter estimation of the human index finger. In Proc. of the IEEEInt. Conf. on Robotics and Automation, pages 223–230, San Diego, May 1994.

[92] M. E. Rosheim. Robot Evolution: The Development of Anthrobotics. John Wiley & Sons, Inc., 1994.

[93] D. De Rossi. Artificial tactile sensing and haptic perception. Meas. Sci. Thec., 2:1003–1016, 1991.

[94] J. K. Salisbury and J. J. Craig. Articulated hands: Force control and kinematic issues. The Int. Journal of Robotics Research, 1(1), Spring 1982.

[95] J. K. Salisbury, Jr. Kinematic and Force Analysis of Articulated Hands. PhD thesis, Stanford University, July 1982.

[96] G. Schlesinger. Ersatzglieder und Arbeitshilfen fur Kriegsbeschadigte und Unfallverletzte, chapter Der Mechanische Aufbau der Kunstlichen Glieder, pages 321–699. Springer, 1919.

[97] Scriptar and F. Ricci. Androids: The Jaquet-Droz Automatons. Scriptar, 1979.

[98] A. Streri. Seeing, Reaching, Touching. The MIT Press, 1993.

[99] D. Taddeucci and P. Dario. Experiments in synthetic psychology for tactile perception in robots: Steps towards implementing humanoid robots. In Proc. of the IEEE Int. Conf. on Robototics and Automation, pages 2262–2267, Leuven, Belgium, May 1998.

[100] D. Taddeucci, P. Dario, and E. Ansari. An approach to anthropomorphic robotics: Guidelines and experiments. In Proc. of the 1999 IEEE/RSJ Int. Conf. on Intelligent Robots and Systems, 1999.

[101] D. Taddeucci, P. Gorce, Y. Burnod, et al. SYNERAGH, a european project on anthropomorphic grasping and handling for humanoid robots. In First IEEE-RAS Int. Conf. on Humanoid Robots, Cambridge, MA, September 2000. IEEE-Robotics and Automation Society.

[102] D. Taddeucci, C. Laschi, P. Dario, F. Leoni, M. Guerrini, K. Cerbioni, and C. Colosimo. Model and implementation of an anthropomorphic system for sensory-motor perception. In Proc. of the 1998 IEEE/RSJ Int. Conf. on Intelligent Robots and Systems, pages 1962–1967, Victoria B.C., Canada, October 1998.

[103] C. L. Taylor and R. J. Schwarz. The anatomy and mechanics of the human hand. Artificial Limbs, 2:22–35, 1955.

[104] S. Venkataraman and T. Iberall. Dextrous Robot Hands. Springer-Verlag, New York, 1990.

[105] F. R. Wilson. Hand: How Its Use Shapes the Brain, Language, and Human Culture. Vintage Books, New York, NY, 1999.

[106] T. Wohlers. Rapid prototyping and tooling state of the industry: 1999 worldwide progress report. Technical report, Wohlers Associates, 1999.

[107] J. Won, K. DeLaurentis, and C. Mavroidis. Rapid prototyping of robotic systems. In Proc. of IEEE Int. Conf. on Robotics and Automation, pages 3077–3082, San Francisco, CA, April 2000.

[108] http://www.jrkerr.com.

[109] Y. Youm, T. E. Gillespie, A. E. Flatt, and B. L. Sprague. Kinematic investigation of normal mcp joint. Journal of Biomechanics, 11:109–118, 1978.